Hydrol. Earth Syst. Sci. Discuss., 12, 5465–5517, 2015
www.hydrol-earth-syst-sci-discuss.net/12/5465/2015/
doi:10.5194/hessd-12-5465-2015

Hydrology and Earth System Sciences
Discussions
Open Access

Sensitivity of water scarcity events to ENSO driven climate variability at the global scale

T. I. E. Veldkamp[1], S. Eisner[2], Y. Wada[3,4,5], J. C. J. H. Aerts[1], and P. J. Ward[1]

[1]Institute for Environmental Studies (IVM), VU University Amsterdam, Amsterdam, The Netherlands
[2]Center for Environmental Systems Research, University of Kassel, Kassel, Germany
[3]Center for Climate Systems Research, Columbia University, New York, USA
[4]NASA Goddard Institute for Space Studies, New York, USA
[5]Department of Physical Geography, Utrecht University, Utrecht, The Netherlands

Received: 6 May 2015 – Accepted: 11 May 2015 – Published: 11 June 2015

Correspondence to: T. I. E. Veldkamp (ted.veldkamp@vu.nl)

Published by Copernicus Publications on behalf of the European Geosciences Union.

Abstract

Globally, freshwater shortage is one of the most important risks for society. Changing hydro-climatic and socioeconomic conditions have aggravated water scarcity over the past decades. A wide range of studies show that water scarcity will intensify in the future, as a result of both increased consumptive water use and in some regions climate change However, less attention has been paid to the impacts of climate variability on water scarcity, despite its importance for adaptation planning. Therefore, we present the first global scale sensitivity assessment of water scarcity and water availability to El Niño–Southern Oscillation (ENSO), the most dominant signal of climate variability.

We show that over the time period 1961–2010, both water availability and water scarcity conditions are significantly correlated with ENSO-driven climate variability over a large proportion of the global land area (> 28.1 %); an area inhabited by more than 31.4 % of the global population. We also found, however, that climate variability alone is often not enough to trigger the actual incidence of water scarcity events. The sensitivity of a region to water scarcity events, expressed in terms of land area or population impacted, is determined by both hydro-climatic and socioeconomic conditions. Currently, the population actually impacted by water scarcity events consists of 39.6 % (water stress) and 41.1 % (water shortage) of the global population whilst only 11.4 % (water stress) and 15.9 % (water shortage) of the global population is at the same time living in areas sensitive to ENSO driven climate variability. These results are contrasted however by differences in found growth rates under changing socioeconomic conditions, which are relatively high in regions affected by water scarcity events.

Given the correlations found between ENSO and both water availability and water scarcity, and the relative developments of water scarcity impacts under changing socioeconomic conditions, we suggest that there is potential for ENSO-based adaptation and risk reduction which could be facilitated by more research on this emerging topic.

1 Introduction

Over the past decades, changing hydro-climatic and socioeconomic conditions have led to increased regional and global water scarcity problems (Alcamo et al., 1997; Kummu et al., 2010; van Beek et al., 2011; van Vliet et al., 2013; Veldkamp et al., 2015; Vorosmarty et al., 2000; Wada et al., 2011a). Freshwater shortage is recognized as one of the most important global risks, not only in terms of likelihood but also with respect to its impacts, with societal and economic consequences that result from the inability to meet water demands (Hanemann, 2006; Howell, 2013; Rijsberman, 2006; Young, 2005). In the near future, projected changes in human water use and population growth – in combination with climate change – are expected to aggravate water scarcity conditions and their associated impacts on society (Alcamo et al., 2007; Haddeland et al., 2014; Kiguchi et al., 2014; Lehner et al., 2006; Prudhomme et al., 2014; Schewe et al., 2014; Sperna Weiland et al., 2012; Stahl, 2001; van Vliet et al., 2013; Wada et al., 2014a).

Whilst a wide range of studies have assessed the role of long-term climate change and changing socioeconomic conditions on past and future global blue water availability and water scarcity events, the impact of inter-annual climate variability is less well understood (Kummu et al., 2014; Lundqvist and Falkenmark, 2010; Rijsberman, 2006; Veldkamp et al., 2015). Taking into account the impact of climate variability relative to longer-term changes in either the socioeconomic or climatic conditions is, however, important as these factors of change may amplify or offset each other at the regional scale (Hulme et al., 1999; McPhaden et al., 2006; Murphy et al., 2010; Veldkamp et al., 2015). Correct information on current and future water scarcity conditions and thorough knowledge on the relative contribution of its driving forces, such as inter-annual variability, help water managers and decisions makers in the design and prioritization of adaptation strategies for coping with water scarcity.

To address this issue, we assess in this paper the sensitivity of blue water resources availability, consumptive water use, and water scarcity events to climate variability driven by El Niño–Southern Oscillation (ENSO) at the global scale over the time period 1961–2010. Moreover, we evaluated whether those areas with found statistically significant correlations have been affected by water scarcity events; if there is a spatial clustering in terms of population or land area affected by water scarcity events and/or population living in areas sensitive to ENSO driven climate variability, and whether this spatial clustering has changed over time given the socioeconomic developments. Within this contribution we investigate the impact of ENSO as it is the most dominant signal of inter-annual climate variability (McPhaden et al., 2006). Also, since ENSO can be predictable with reasonable skill up to several seasons in advance (Cheng et al., 2011; Ludescher et al., 2014), this can provide useful information for adaptation management to account for inter-annual variability in water resources and water scarcity estimates, enabling the prioritization of adaptation efforts in the most affected regions ahead of those extreme events (Bouma et al., 1997; Cheng et al., 2011; Dilley and Heyman, 1995; Ludescher et al., 2013; Ward et al., 2014a, b; Zebiak et al., 2014).

ENSO is the result of a coupled climate variability system in which ocean dynamics and sea level pressure interact with atmospheric convection and winds (ocean–atmosphere feedback mechanisms). El Niño is the oceanic component, whereby waters over the eastern equatorial Pacific Ocean reach anomalously high temperatures. This eastern Pacific Ocean surface is relatively cool under neutral conditions, while it reaches anomalously low temperatures during La Niña conditions. The Southern Oscillation is the atmospheric component, represented by the east–west shifts in the tropical atmospheric circulation between the Indian and West Pacific Oceans and the East Pacific Ocean (Kiladis and Diaz, 1989; Parker et al., 2007; Rosenzweig and Hillel, 2008; Wallace and Hobbs, 2006; Wang et al., 2004). ENSO is well-known for its impacts on both average river flows and hydrological extremes (peak and low flows) at local and regional scales (e.g. Chiew et al., 1998; Kiem and Franks, 2001; Lü et al., 2011; Mosley, 2000; Moss et al., 1994; Piechota and Dracup, 1999; Räsänen and Kummu, 2013; Whetton et al., 1990). Several studies have also examined ENSO's impact at the global scale (Chiew and McMahon, 2002; Dettinger et al., 2000; Dettinger and Diaz, 2000; Labat, 2010; Sheffield et al., 2008; Ward et al., 2010, 2014a) with only a limited number of studies assessing the societal impacts (e.g. in terms of population affected, GDP loss, or with respect to human health) of hydrological extremes under the different ENSO stages at the global scale (Bouma et al., 1997; Dilley and Heyman, 1995; Kovats et al., 2003; Rosenzweig and Hillel, 2008; Ward et al., 2014b). To the best of our knowledge, none of these studies have executed a global-scale assessment of the sensitivity of water resources availability, consumptive water use patterns, and water scarcity events to ENSO.

2 Methods

In short, we carried out this assessment through the following steps: (1) used daily discharge and runoff time-series (0.5° × 0.5°) from an ensemble of three global hydrological models (WaterGAP, PCR-GLOBWB, and STREAM) (Sect. 2.1); (2) combined time-series of water availability, consumptive water use and population to calculate water scarcity conditions for the period 1961–2010 (Sects. 2.2–2.4); (3) identified statistical relationships between water availability, consumptive water use and water scarcity conditions, and indices of ENSO (Sect. 2.5.1); and (4) evaluated whether the areas with significant correlations with ENSO are actually affected by water scarcity events, how the impacts (population and land area affected) are clustered, and how the impacts have changed through time. Modelling uncertainty was evaluated by comparing the results from the ensemble-mean time-series with the outcomes of the individual global hydrological models (Sect. 2.6).The following paragraphs describe our methods in detail.

2.1 Ensemble mean monthly runoff and discharge

We simulated global gridded daily discharge and runoff over the period 1960–2010 at a resolution of 0.5° × 0.5° using three global hydrological models: PCR-GLOBWB (van Beek et al., 2011; Wada et al., 2014b), STREAM (Aerts et al., 1999; Ward et al., 2007) and WaterGAP (Muller Schmied et al., 2014), forced with WATCH Forcing Data – ERA Interim (WFDEI) daily precipitation and temperature data (0.5° × 0.5°) (Weedon et al., 2014) for the period 1979–2010 and WATCH forcing data ERA40 (WFD) for the period 1960–1978 (Weedon et al., 2011). In order to compensate for offsets in long-term radiation fluxes between the two datasets, as found by Müller Schmied et al. (2014), WFD down-welling shortwave and longwave radiation were adjusted for use in WaterGAP to WFDEI long-term means following the approach of Haddeland et al. (2012). Daily values were aggregated to time-series of monthly discharge and runoff. Using global hydrological models gives us the advantage of a global coverage whereas the portfolio of observed datasets (water availability and consumptive water use) is bounded by its biased regional distribution (Hannah et al., 2011; Ward et al., 2010, 2014a). However, we are aware of the caveats using these types of models to estimate water availability as all large-scale hydrological models have their own strengths and shortcomings (Gudmundsson et al., 2012; Nazemi and Wheater, 2015a, b). Therefore, we constructed ensemble-mean time-series of both monthly discharge and runoff capturing the three global hydrological models. The results of the individual modelling efforts were used to evaluate the modelling agreement (Sects. 2.4 and 3.5).

2.2 Calculating water availability

Water availability is expressed in this paper as the sum of monthly runoff per grid-cell and Food Producing Unit (FPU). FPUs represent a hybrid between river basins and economic regions within which water scarcity issues can be solved internally (Cai and Rosegrant, 2002; de Fraiture, 2007; Kummu et al., 2010; Rosegrant et al., 2002). We used here an updated version of the FPUs used by Kummu et al. (2010), which consists of 436 FPUs, excluding small island FPUs. For grid-cells or FPUs located within one of the world's larger river basins we redistributed runoff in order to avoid local over- or under-estimations in water availability. Runoff was redistributed across the grid-cells within these larger river basins, proportionally to the discharge distribution of that large river basin (Gerten et al., 2011; Schewe et al., 2014):

$$\mathrm{WA}_i = \frac{\mathrm{R_b} \cdot \mathrm{Q}_i}{\sum \mathrm{Q}_i}, \tag{1}$$

whereby WA_i is the monthly water availability within grid-cell i, R_b is the total monthly runoff within large river-basin b, Q_i is the monthly discharge in grid-cell i, and $\sum Q_i$ is the sum of the monthly discharge over all cells within large river-basin b.

Subsequently, we calculated the annual water availability by aggregating the simulated ensemble-mean monthly water availability time-series using hydrological years, both at the grid-cell and FPU level. The use of hydrological years is necessary in this assessment as ENSO tends to develop to its fullest strength during the period December–February, which intersects with the standard calendar year boundaries (Ward et al., 2014a, b). Hydrological years are referred to by the year in which they end, e.g. hydrological year 1961 refers here to the period October 1960–September 1961. Within this study we follow Ward et al. (2014a) and distinguish two hydrological years on the basis of long-term monthly maximum water availability per river basin: October–September (standard) and July–June (for river basins that have their long-term monthly maximum water availability in September, October or November). The river basin delineation used here was derived from the WATCH project (Döll and Lehner, 2002) and is equal to the river basin delineation that is used as the input for the FPU classification used within this study. We used the hydrological years setting determined at grid-level, using the WATCH river-basins, as input for the distinction between hydrological years at FPU scale. If an FPU consisted of more than one river basin we based the choice of hydrological year on the month (with long-term maximum water availability) with the highest prevalence within this FPU. Figure A1 shows for both the grid-cell level and FPU-scale the hydrological year distinction as used within this study.

2.3 Calculating consumptive water use

Time-series of monthly consumptive water use ($0.5^\circ \times 0.5^\circ$) were estimated for the sectors: livestock, irrigation, industry and domestic within PCR-GLOBWB, being forced with daily WFD-EI precipitation and temperature data (Wada et al., 2014b, 2011b). Time-series of desalinated water use and non-renewable ground water abstractions were subtracted from the total consumptive water use estimates as they lower the need for blue water. Subsequently we aggregated gridded monthly consumptive water use into yearly totals per FPU ($\mathrm{WC}_{i,\mathrm{yr}}$), following the hydrological years. Since the resulting "transient" consumptive water use estimates are partially driven by changing socio-economic conditions (population, GDP and growth in irrigated areas) and therefore disguise any possible correlations with ENSO driven climate variability, we repeated the steps above whilst we fixed the socioeconomic parameters at 1961 levels (following the hydro-year naming convention). These "fixed" consumptive water use estimates were used to evaluate the sensitivity to ENSO driven climate variability (Sects. 3.1 and 3.2) whereas the "transient" water consumption time-series were used to evaluate the development of water scarcity conditions under changing socioeconomic conditions (Sect. 3.3).

2.4 Calculating water scarcity conditions

Within this study we applied two complementary indicators to express water scarcity conditions per FPU: the Water Crowding Index (WCI) for population-driven water shortage and the Consumption-to-Availability ratio (CTA-ratio) for demand-driven water stress (Brown and Matlock, 2011; Rijsberman, 2006). The WCI quantifies the yearly water availability per capita (Falkenmark, 1986, 2013), whereby water requirements are based on household, agricultural, industrial, energy and environmental water consumption (Rijsberman, 2006). Like previous studies (e.g. Arnell, 2003; Kummu et al., 2010), we used 1700 m^3 capita per year as the threshold level to evaluate water shortage events. The CTA-ratio evaluates the ratio between water consumed and water availability in a specific region and is the most used indicator for water stress assessments (e.g. used in Wada et al., 2011a; Hoekstra et al., 2012; Kiguchi et al., 2014; Vorosmarty et al., 2000; Oki and Kanae, 2006; Falkenmark, 2013a;). In line with earlier studies (Hoekstra et al., 2012; Kiguchi et al., 2014; Veldkamp et al., 2015; Wada et al., 2011a), a threshold level of 0.2 was used here to indicate water stress events. Equations 2 and 3 show the use of the WCI ($\mathrm{WCI}_{i,\mathrm{yr}}$) and the CTA-ratio ($\mathrm{CTA}_{i,\mathrm{yr}}$), respectively:

$$\mathrm{WCI}_{i,\mathrm{yr}} = \frac{\mathrm{WA}_{i,\mathrm{yr}}}{\mathrm{P}_{i,\mathrm{yr}}} \quad (\text{water shortage event if } \mathrm{WCI}_{i,\mathrm{yr}} \leq 1700), \tag{2}$$

$$\mathrm{CTA}_{i,\mathrm{yr}} = \frac{\mathrm{WC}_{i,\mathrm{yr}}}{\mathrm{WA}_{i,\mathrm{yr}}} \quad (\text{water stress event if } \mathrm{CTA}_{i,\mathrm{yr}} \geq 0.2), \tag{3}$$

whereby $\mathrm{WA}_{i,\mathrm{yr}}$ is the water available per spatial unit i and hydrological year yr, $P_{i,\mathrm{yr}}$ is the population, and $\mathrm{WC}_{i,\mathrm{yr}}$ is consumptive water use. Water scarcity conditions were assessed here at the FPU-scale. The FPU scale is seen as an appropriate spatial scale to study water scarcity conditions as lower-scale water scarcity issues can be overcome by the reallocation of water demand and supply within this spatial unit (Kummu et al., 2010). However, one should keep in mind that, due to the assumption of full exchange possibilities – both from an infrastructural and water management perspective – and its relative large spatial scale, analysis executed at the FPU-scale may disguise lower-scale water scarcity issues (Kummu et al., 2010; Wada et al., 2011a).

The population data used for the calculation of the WCI (Eq. 2) were adopted from Wada et al. (2011a, b), who derived yearly gridded population maps ($0.5^\circ \times 0.5^\circ$) from yearly country-scale FAOSTAT data in combination with decadal gridded global population maps (Klein Goldewijk and van Drecht, 2006). We aggregated these gridded population maps to FPU-scale for use in this study. In line with the hydrological year naming convention, population estimates were used for the year in which the hydrological year ends, e.g. for hydrological year 1961 we used population estimates of 1961 as input for the WCI and to calculate water scarcity impacts.

2.5 Sensitivity of water availability, consumptive water use, and water scarcity conditions to ENSO driven climate variability

At the grid-cell level, we examined the relationship between water availability and water consumption, and ENSO driven climate variability by means of their correlation with the Japan Meteorological Agency's (JMA) Sea Surface Temperature (SST) anomaly index (http://coaps.fsu.edu/jma, ftp://www.coaps.fsu.edu/pub/JMA_SST_Index/). We used here three-monthly mean values of the JMA SST over the periods October–December, November–January, December–February, and January–March, as El Niño and La Niña expressions are strongest in these months (Dettinger and Diaz, 2000). Following Ward et al. (2014b), we examined the correlation between WA_{ann} and WC_{ann}, and the 3-monthly mean JMA SST value (OND, NDJ, DJF, JFM), using Spearman's rank correlation coefficient Rho. Significance was assessed by means of regular bootstrapping ($n = 1000$, $p = 0.05$) while field significance for each of the 3-monthly JMA SST correlation values was tested using the binomial distribution (Livezey and Chen, 1982). Subsequently, we assessed at the scale of FPUs the relationship between water scarcity conditions, and ENSO driven climate variability. Again, the three-monthly mean values of the JMA SST over the periods October–December, November–January, December–February, and January–March were used to calculate Spearman's Rho correlation coefficients, while we tested significance using regular bootstrapping ($n = 1000$, $p = 0.05$). Moreover, we examined the percentage anomalies in the median values of water scarcity conditions between El Niño (EN) and La Niña (LN) years, compared to the median values under all years. To distinguish between El Niño, La Niña and neutral years we used the classification of ENSO years from the Center for Ocean–Atmospheric Prediction Studies based on the JMA SST values (http://coaps.fsu.edu/jma.shtml). Years are assigned as El Niño or La Niña years when their 5 month moving average JMA SST index values are (–)0.5 °C or greater (El Niño)/smaller (La Niña) for at least six consecutive months (including October–December). Reference to the different ENSO years was adjusted to be consistent with the naming convention used for the hydrological years (Table 1). We used a bootstrapped version of the non-parametric Mann–Whitney U test ($n = 1000$, $p = 0.05$) to test the statistical differences in median values.

The critical threshold-values put in place for the WCI and the CTA-ratio (here: 1700 and 0.2 respectively) determine whether water scarcity conditions adversely affect population or society. Per FPU we therefore evaluated which percentage of land-area in which there is a correlation between ENSO and water scarcity conditions, are also affected by water scarcity events; how population is clustered in these areas compared to the general pattern of population density; and how these numbers changed through time given the changing socioeconomic conditions, relative to developments in: (1) the population and land-area sensitive to ENSO driven climate variability but not affected by water scarcity events; (2) the population and land-area affected by water scarcity events, in areas that lack a significant correlation with ENSO driven climate variability; and to (3) the total population growth.

2.6 Evaluating modelling uncertainty

A cross-model validation was executed in order to evaluate the modelling uncertainty whereby we compared the results from the ensemble-mean with the outcomes of the individual global hydrological models. We examined the agreement among the different modelling results and the ensemble-mean when looking at: (1) the sensitivity of water availability and water scarcity conditions to ENSO driven climate variability; and (2) the impacts of water scarcity events and relation to ENSO driven climate variability under changing socioeconomic conditions.

3 Results

In this section, we first demonstrate how water availability and consumptive water use correlate with ENSO driven climate variability at the grid-cell level, keeping the socioeconomic conditions fixed at 1961 levels (Sect. 3.1). Subsequently, we show how sensitive water scarcity conditions are to ENSO driven climate variability (Sect. 3.2). Finally, we evaluate whether those areas with statistically significant correlations are actually affected by adverse water scarcity conditions, and discuss how these shares change over time under socioeconomic developments.

3.1 Sensitivity of water availability and consumptive water use to ENSO driven climate variability

Significant correlations of water availability to variations in JMA SST were found across 24.1 % of the land surface (excluding Greenland and Antarctica). For consumptive water use, we found 3.1 % of the land surface to be significantly correlated with yearly variations in JMA SST. Using the 3-monthly JMA SST period with the highest correlation, Fig. 1 shows for both water availability and consumptive water use its correlation coefficient with the inter-annual variation in the 3-monthly average JMA SST values at the grid-cell level. Only those correlations which reach statistical significance at a 5 % confidence interval are shown here. Field significance was tested for the individual 3 month correlation results and found to be highly significant when looking at water availability ($p < 0.01$) but insignificant when considering consumptive water use ($p > 0.5$). In Fig. A2 (Appendix) we present the results at FPU scale, and in Fig. A3 we show the results for all FPUs (irrespective of statistical significance). At this scale of FPUs, we found percentage of total land area with significant correlations of 37.1 % for water availability and 8.3 % for consumption water use.

Regions well-known for their correlation of hydrological extremes with ENSO variability (both peak discharges and low-flows) also have a statistically significant correlation between ENSO and annual total water resources availability. When comparing our results to previous studies (e.g. Dettinger and Diaz, 2000; Ward et al., 2010, 2014a), we find corresponding significant correlations in the regions mid-west North-America, the Caribbean, Latin America, Southern Africa, South–East and Central Asia and the Pacific. Moreover, the sign of the correlations found within four large river basins in Latin America and Africa, (Amazon Congo, Paraná, and Nile) is supported by earlier estimates of Amarasekera et al. (1997) who assessed the correlation between ENSO and the natural variability in the flow of tropical rivers. Significant correlations as shown for other regions were also found in case studies focusing on Northern America (e.g. Clark II et al., 2014; Schmidt et al., 2001), Southeast Asia (e.g. Lü et al., 2011; Räsänen and Kummu, 2013), Southern Africa (e.g. Meque and Abiodun, 2014; Richard et al., 2001), and Australia (e.g. Chiew et al., 2011; Dutta et al., 2006). Positive correlations, i.e. more water available with the JMA SST index moving towards El Niño values, were found for 8.5 % (13.2 %) of the global land surface, as measured at the grid-cell (FPU) level, while negative correlations were found in basins covering 15.6 % (23.9 %) of the global land surface. The spatial variation in sign of the found correlation is in line with the results of Ward et al. (2014a), who found that annual flood and mean discharge values intensify under La Niña and decline when moving towards El Niño phases globally in more areas than the other way around. When looking at consumptive water use we found positive significant correlations for only 0.6 % (1.0 %), and negative correlations for 2.5 % (7.3 %) of the global land surface (Fig. 1a). In line with earlier research (e.g. Meza et al., 2004; Islam and Gan, 2015) we would have expected to find more areas with a significant correlation between consumptive water use and ENSO driven climate variability. A number of explanations could be given for the absence of significant correlations patterns in this study: (1) the consumptive water use estimates used in this study are calculated by means of multiple socioeconomic and hydro-climatic proxies and variables, such as extent of irrigated areas, number of livestock, GDP, (long-term mean) monthly temperatures, and precipitation estimates, and should be interpreted as potential consumptive water use; (2) of these variables only irrigation water use could be linked directly to ENSO driven climate variability by means of its temperature and precipitation input variables. “Fixed” consumption numbers in other sectors might attenuate therefore the variability found within the irrigation sector; (3) climate-driven variations in irrigation water demands are the result of changes in crop evapotranspiration and changes in green water availability, which do not have a univocal relation with ENSO driven climate variability at all times, but are partly determined by the month-specific cropping calendar and antecedent conditions, such as the memory of the soil; and (4) yearly totals of consumptive water use were applied in this study to assess its sensitivity to ENSO driven climate variability whereas it might be more appropriate for consumptive water use to assess its correlation either using monthly time-scales or yearly maxima.

3.2 Sensitivity of water scarcity conditions to ENSO driven climate variability

Subsequently, we assessed how sensitive water scarcity conditions, measured at the FPU-scale, are to ENSO driven climate variability. Significant correlations to variations in JMA SST were found for 28.1 and 37.9 % of the land surface area when using the CTA-ratio (water stress) and WCI (water shortage) respectively, while being tested under a 5 % confidence interval. Due to the clustering of population and consumptive water use we found even higher percentages when looking at the population living in these areas, 31.4 and 38.7 % of the global population in 2010 for the CTA-ratio and WCI respectively. Figure 2 shows the areas with a significant positive (red) or negative (blue) correlation of water stress conditions (CTA-ratio) with the variation in JMA SST values, using the 3-monthly JMA SST period with the highest correlation (JMA $\text{SST}_{\text{bestoff}}$). Correlation results found for water shortage conditions, as defined by the WCI, are shown in Fig. A4. This figure shows a similar pattern, and in line with the correlations for the annual water availability estimates, we found that for the majority of the land area with a significant correlation, water scarcity conditions (both CTA-ratio and WCI) become more severe when the JMA SST index moves towards El Niño values, for 16.8 and 23.9 % of the land surface area for water stress and water shortage, respectively.

The regional variation in sensitivity of water scarcity conditions to ENSO driven variability (Figs. 2 and A4) is clearly driven by the spatial distribution of water availability correlations as the general patterns are similar to those found in Fig. 1. The unequal clustering of water availability and consumptive water use leads, however, in some regions to a strengthening or weakening of the correlation signal, for example when comparing the regional variation in sensitivity results for water stress within the Amazon basin or in Southern Africa (Fig. 2) with the regional variation in correlation results for water availability as found in Fig. A2. For a selection of FPUs, we found significant correlations for both water availability and consumptive water use, while they lack significant correlations when considering water stress conditions, and vice versa. In Southeast Asia (Fig. 3), for example, we observed significant correlations between ENSO and water availability and consumptive water use, but no significant correlations between ENSO and water stress. One explanation for this observation could be that if both water availability and consumptive water use increase or decrease with more or less the same strength under changing JMA SST values, the net effect on the CTA-ratio could be insignificant since the ratio between both variables remains equal. When using the WCI, we did not find any FPUs with (in)significant correlations for water availability, and vice versa for water shortage conditions. This could be explained by the fact that the WCI is only driven by changes in water availability and population growth, of which the latter factor was fixed in this analysis. Moreover, for all the FPUs with a significant correlation of water availability with varying JMA SST values, none of them lacks a correlation for the WCI due to the absence of population in this area (which would result in continuously infinite scarcity values when applying the WCI).

Significant anomalies ($p = 0.05$, tested by regular bootstrapping $n = 1000$) in water scarcity conditions under El Niño and La Niña years, compared to all years, were found for 12.8 and 14.8 % of the global land area using the CTA-ratio and the WCI respectively, see Figs. A5 and A6 in the Appendix. These numbers could be split into 3.4 % showing significant anomalies under El Niño years, 12.8 % under La Niñ a years, and 3.4 % under both ENSO phases for water stress conditions (Fig. A5), and 6.9 % (El Niño phase), 9.5 % (La Niña phase), and 1.6 % (both EN and LN phase) for water shortage conditions (Fig. A6). Not all regions with a significant anomaly under El Niño years show (significant) anomalies in the opposite direction during La Niñ a years. For example, Fig. 4 visualizes the asymmetry in the anomalies found during the El Niño and La Niña phase for Latin America. Moreover, areas with significant correlations with the JMA SST index do not always show significant anomalies when looking at the different ENSO phases. This could be explained by the fact that only those years for which the 5 month moving average JMA SST index values are (–)0.5 °C or greater (El Niño)/smaller (La Niña) for at least six consecutive months (including October–Dec) are assigned as El Niño or La Niña years (see Sect. 2.5). Using this ENSO year definition thus disguises all variability in JMA SST values that falls just below the threshold set, variation that can have a significant effect on water scarcity conditions however. Therefore we continue our analysis with the correlations found for the JMA SST index values.

3.3 Sensitivity of water scarcity events to ENSO driven climate variability under changing socioeconomic conditions

Whether those areas with significant correlations are actually in water scarcity requires a certain combination of water availability and consumptive water use (CTA-ratio) or population density (WCI). If water scarcity conditions do not approach the critical threshold levels for water scarcity, no critical water scarcity situation emerges. Although inter-annual variation in water availability determines for a large share the size and significance of variability in water scarcity conditions, it is thus only in combination with the "right" socioeconomic conditions that it can be decisive considering the actual incidence of water scarcity events (Veldkamp et al., 2015).

Figure 5 shows per FPU the frequency of water stress events ($CTA \geq 0.2$). Over the period 1961–2010, 23.1 % of the total land surface was affected by water stress events, varying from being affected only once up to permanently being under influence of adverse water scarcity conditions. At the same time, we found significant correlations to variations in JMA SST values for one-third (33.1 %) of the land area susceptible to water stress events (blue dots). The global results found under the WCI ($WCI \leq 1700$) are roughly similar, although the spatial distribution of affected land varies significantly due to the unequal clustering of population and consumptive water use (Fig. A7). Using the WCI, up to 23.1 % of the total land surface area has been affected by water shortage events at least once over the period 1961–2010 whilst 44.2 % of this selected land area shows variations in water shortage conditions that could be significantly correlated to ENSO driven climate variability (blue dots). Percentages of population affected by water scarcity events are globally a factor 2.8 higher than the share of land area affected when using the CTA-ratio, with 39.6 % of the global population being affected by water scarcity events in 2006–2010 respectively (using 5 year averaged values), compared to 13.9 % of the global land area. Similar results were found under the WCI, 41.1 % of the global population was affected by water scarcity events in 2006–2010 (using 5 year averaged values), compared to 13.9 % of the total land area which is equal to a factor difference of 2.9.

Due to the socioeconomic developments over the period 1961–2010 water scarcity conditions and impacts intensified, both in absolute and relative sense. Figure 6 shows for the CTA-ratio (water stress) these increases in population and land area affected (red + orange fill) under changing socioeconomic conditions over the period 1961–2010 and at the global scale, relative to the total population and land area (dashed lines, set at 100 in 1961), and the development in population and land areas with a significant correlation to ENSO driven climate variability (grey + red fill). Similar graphs for the WCI (water shortage) are shown in Fig. A8. From 1961 to 2010, using 5 year averaged values, the total global population increased with a factor 2.1 (from 2.97 billion to 6.25 billion). At the same time, we found increases in the global population affected by water scarcity events. When using the CTA-ratio we found a factor difference of 5.5 (from 0.45 billion to 2.47 billion), for the WCI we found increases of a factor 6.6 (from 0.39 billion to 2.57 billion). In relative sense, the population affected by water scarcity events increased from 13.2 and 15.3 % up to 41.1 and 39.6 %, when looking at the WCI and CTA-ratio respectively. Unequal growth rates and the spatial clustering of population and consumptive water use impact water scarcity events and its consequences given the fact that the share of land area affected by water scarcity events only doubled (factor: 2.2) over this same period for the CTA-ratio, while it increased with a factor 4.7 when looking at the WCI.

Although the share of population sensitive to ENSO driven climate variability increased with a factor 2.3 (WCI) to 2.4 (CTA-ratio) at the global level, it remained rather equal over time when considered relative to the growth in total population, with relative growth factors of 1.1 using both the CTA-ratio (from 28.7 to 31.3 %) and the WCI (from 34.1 to 38.7 %). The population sensitive to ENSO variability and living in areas affected by water scarcity events currently represent only a minority of the global population, 15.9 % for the WCI and 11.4 % when using the CTA-ratio. However, these results are contrasted with relative high growth factors, 3.5 and 1.7 for the CTA-ratio, and 6.9 and 3.3 for the WCI, representing the absolute and relative (with respect to the total population growth) increases over time respectively.

Regional variations in the population affected by water stress and/or being sensitive to ENSO driven climate variability under changing socioeconomic conditions, are visualized in Fig. 7. Although these regional figures do not lend themselves to a similar growth factor analysis such as executed on the global numbers in Fig. 6, we can distinguish by means of visual inspection different characteristic region-types. The first group of regions (Latin America Australia and the Pacific, the Caribbean, and Middle and Southern Africa) experiences significant correlations with ENSO variability for a relative large share of its land area and population (≥ 25 % of the total population in 2010) whilst water scarcity impacts are low (< 25 % of the total population affected in 2010). The second group of regions shows both a relatively low sensitivity to ENSO driven climate variability (< 25 % of the total population in 2010) and low water scarcity impacts (< 25 % of the total population in 2010), e.g. Northern America and Western Europe. For the third group of regions (the Middle East, India, Southeast Asia, and West and Central Asia) we find significant water scarcity impacts (≥ 25 % of the total population in 2010) but no or relative low sensitivity to ENSO variability (< 25 % of the total population in 2010). Finally, the fourth group of regions shows relatively high water scarcity impacts in terms of population affected (≥ 25 % of the total population in

2010) and abundant sensitivity to ENSO driven climate variability (≥ 25 % of the total population in 2010), e.g. China and Northern Africa. Comparing these observations with the regional figures found for water shortage events (Fig. A9), assessed by means of the WCI, we found different results for the regions West and Central Asia (relative high sensitivity to ENSO variability and relative low water scarcity impacts), and Middle and Southern Africa, the Middle East and Southeast Asia (both experiencing relative high sensitivity to ENSO variability and high water scarcity impacts). Using both water scarcity metrics (i.e. CTA-ratio and WCI) in combination with the observed growth rates in population and population affected by water scarcity events enables us to identify those regions where adaptation measures such as ENSO-based forecasting have the largest (future) potential in coping with and possibly reducing the adverse impacts of water scarcity events: the Caribbean, Latin America, Western and Central Asia, Middle and Southern Africa, Northern Africa, the Middle East, China, Southeast Asia and Australia and the Pacific.

3.4 Cross-model validation

The cross-model validation exercise, in which we compared the outcomes of the individual global hydrological models with their ensemble mean results, shows that our findings considering the sensitivity of water availability, water consumption and water scarcity conditions to ENSO driven climate variability are robust to the use of different hydrological models. When looking at the percentage land area that shows a significant correlation between water availability and variations in JMA SST (Fig. 8) we find for 35.9 % of this selected area that all the individual GHMs show a significant correlation to variations in JMA SST in the same direction as the correlation results found under the ensemble-means whilst the found correlations under the ensemble-mean are supported by at least two global hydrological models for 72.3 % of this land area.

A comparison of the individual modelling results with the ensemble-mean in terms of the estimated population affected by water scarcity events and/or living in areas sensitivity to ENSO driven climate variability reveals the size of inter-model deviations at the global scale with respect to estimated impacts and their developments over time (Fig. 9). Looking at the 2010 values, we find the smallest percentage difference between models in the estimates of the population affected by water scarcity events (+17.2 % CTA-ratio, +21.8 % WCI), and the largest variations when looking at the population both affected by water scarcity events and living in areas sensitive to ENSO driven climate variability (+68.9 % CTA-ratio, +54.2 % WCI). Percentage deviations are smaller when considering land area affected rather than the population affected (Fig. A10). As shown in Figs. 9 and A10, the inter-model comparison reveals that the impact estimates of the ensemble-mean are conservative when comparing them with the individual modelling results, especially when looking at the population or land area sensitive to ENSO variability and/or being affected by water scarcity events.

4 Discussion

Within this study we found that both water resources availability and water scarcity conditions can be significantly correlated with ENSO driven climate variability as measured with the JMA SST index for a relative large share of the global land area. Due to the clustering effects we found even larger shares when looking at the population living in these areas. The analysis presented in this study also reveals, however, that inter-annual variability itself, such as the ENSO driven climate variability, is often not enough to cause water scarcity events to actually occur. We found that it is a combination of multiple hydro-climatic factors, such as the mean water resources availability and its inter-annual variability around the mean, together with the prevalent socioeconomic conditions, that determines the susceptibility of a region to water scarcity events, a finding earlier suggested by Veldkamp et al. (2015) and Wada et al. (2011a), and its implications being discussed in Hall and Borgomeo (2013). The actual impact of water scarcity events depends, moreover, not only on the number of people affected or the severity of a water scarcity event itself, but on how sensitive this population is to water scarcity conditions, whether and how efficiently governments can deal with water scarcity problems, and how many (financial and infrastructural) resources are available to cope with these water scarce conditions (Grey and Sadoff, 2007; Hall and Borgomeo, 2013).

Given the substantial share of land area, and the even higher rates of population, for which water resources availability and water scarcity conditions show significant correlations with ENSO driven climate variability there is a large potential for ENSO based adaptation and risk reduction to cope with water scarcity and its associated impacts. The relative importance of ENSO driven climate variability in the year-to-year-variability as found in this study could assist water managers and decisions makers in the design of adaptation strategies, such as in optimizing the use of existing reservoir facilities in Australia (Sharma, 2000). Moreover, the potential predictability of ENSO with lead times up to several months, may help in the prioritization of (ex ante) efforts in disaster risk reduction, such as pre-stocking foods and disaster relief goods or crop insurance systems based on ENSO indices (Coughlan de Perez et al., 2014a, b; Dilley, 2000; Suarez et al., 2008). Potential added value of adaptation measures targeting on the impacts of inter-annual variability is high, as it is especially this variability that people find difficult to cope with (Smit and Pilifosova, 2003).

To get more insight in the expected correlation between ENSO, and water resources and scarcity conditions under longer-term climate change and socioeconomic developments, future research could use extreme JMA SST values as a test case in combination with the correlation values found to extrapolate the water resources and scarcity conditions under extreme events. Recent research showed that these extreme ENSO events may become more recurrent in the future (Cai et al., 2014; IPCC, 2013; Power et al., 2013), the uncertainty among the different climate models is, however, large and any agreement on the attribution of long-term climate change to increases in the sensitivity and frequency of ENSO events lacks (Van Oldenborgh et al., 2005; Paeth et al., 2008; Guilyardi et al., 2009). Considering a continuous increase in population growth and water scarcity impacts in the future, hotspots could be appointed that have to deal with water scarcity events and/or are sensitive to ENSO driven variability at the same time. One should take into account, however, that we assumed in this study that the found correlations between water availability, consumptive water use and water scarcity conditions, and the JMA SST index value remains stationary over time. In reality, the strength of correlations between hydrological parameters and ENSO can change over time (Ward et al., 2014a). Further research is therefore needed to assess whether, how much, and in which direction these observed correlation values change under the combination of changing climatic conditions and historic and future socio-economic developments.

The results presented in this study underpin the need for more research on the topic of ENSO and water scarcity, for example regarding the variability in consumptive water use and its correlations with ENSO driven variability, but also considering the potential economic impacts of water scarcity events. Moreover, ENSO is part of an ocean-atmospheric climate variability system that constitutes of many more sub-regional systems and local circulation patterns (e.g. Indian Monsoon and European weather systems) which modulate ENSO signal. New research should look into the sensitivity of water resources availability and scarcity conditions to combinations of these systems.

Finally, future research should focus in the following directions to improve/extend the analysis carried out in this study. In this paper we looked at naturalized flows, no reservoirs or inter-basin transfers were taking into account. Future research should evaluate whether water trading and water storage mechanisms are effective in reducing water scarcity conditions and whether management could be optimized using ENSO-forecasting parameters: e.g. ex ante storage or release of water to counterbalance the impacts of ENSO variability or the incorporation of ENSO variability in water transfer mechanisms, and finally at what costs? Moreover, no management decisions with respect to water saving measures have been taken into account. This could lead to substantial overestimations of the water scarcity conditions as presented in this study. Variability in water demand as observed within this study is based on physical parameters, whilst in reality well-organized societies can react to emerging water scarcity conditions, thereby diminishing their adverse impacts. In other less-well organized regions, we might underestimate water scarcity impacts, as ill-management might prohibit a full and optimal exploitation of the available water resources in space and time, as assumed in this study. Global assessment studies, such as the one presented in this study, are well able to identify the global-scale patterns in water scarcity conditions and sensitivity to ENSO driven climate variability. These types of studies are well-suited for first-order problem definition or the large-scale prioritization of adaptation efforts, such as making a first distinction in regions were ENSO forecasting might be beneficial. When interpreting these assessments one should keep in mind however, that these studies should always be complemented with local or regional scale analyses to assess the actual level of water scarcity "on the ground", their (economic) consequences, and regional or local scale potential for ENSO forecasting as adaptation strategy to cope with water scarcity events.

5 Conclusions

In this paper, we executed the first global scale sensitivity assessment of blue water resources availability, consumptive water use, and water scarcity events to ENSO driven climate variability over the time period 1961–2010. An ensemble-mean of three global hydrological models was used to estimate per FPU the yearly water resources availability and water scarcity conditions, considering both water shortage and stress. Correlations between ENSO, and water resources, water consumption and water scarcity conditions were determined using the JMA SST indices and ENSO phase determination whilst the sensitivity of water scarcity events to ENSO driven climate variability was assessed applying critical threshold values for both water shortage and stress. Finally, the sensitivity of water scarcity events to ENSO driven climate variability under changing socioeconomic conditions was evaluated opening the discussion on their implications for ENSO based adaptation and risk reduction.

Throughout this paper we have shown that water scarcity conditions become more extreme under El Niño and La Niña phases due to the sensitivity of water resources availability and consumptive water use to ENSO driven climate variability. We found that both water resources availability and water scarcity conditions can be significantly correlated with ENSO driven climate variability as measured with the JMA SST index for a relative large proportion (> 28.1 %) of the global land area. Due to the spatial clustering of population and consumptive water use we found even larger shares (> 31.4 % of the total population in 2010) when looking at the population living in these areas. The sensitivity of a region to water scarcity events, expressed in terms of land area or population impacted, is determined by both hydro-climatic and socioeconomic conditions. The results on the impacts of water scarcity events presented in this study provided mixed signals. We found that the population that is currently affected by water scarcity events consists of less than half of the global population (39.6 and 41.1 % for water stress and water shortage events respectively), whilst the population sensitive to ENSO variability and living in areas affected by water scarcity events represent only a minority of the global population, 11.4 and 15.9 % for the water stress and shortage respectively. These results are, however, contrasted by relative differences in growth rates under changing socioeconomic conditions, which are higher in regions affected by water scarcity events than in regions that do not experience any water scarcity.

Given the found correlations of water availability and water scarcity conditions with ENSO driven climate variability, and seen the developments in the population and land area affected by water scarcity events and/or being sensitive to ENSO driven variability under changing socioeconomic conditions, we found that there is large potential for ENSO based adaptation and risk reduction to cope with water scarcity and its associated impacts. The observed regional variations could thereby accommodate in a first-cut prioritization of the implementation of such adaptation strategies. Moreover, the results presented in this study show that there is both potential and need for more research on the issue of ENSO and water scarcity with emerging topics related to the economic impacts of water scarcity; the assessment of consumptive water use and its temporal variability; the combined impact of large scale oscillation systems on water resources and water scarcity conditions; and the transferability of global scale insights to local-scale implications and decisions.

References

Aerts, J. C. J. H., Kriek, M., and Schepel, M.: STREAM (Spatial Tools for River Basins and Environment and Analysis of Management Options): “Set up and requirements”, Phys. Chem. Earth Pt. B, 24, 591–595, 1999.

Alcamo, J., Döll, P., Kaspar, F., and Siebert, S.: Global Change and Global Scenarios of Water Use and Availability: An Application of WaterGAP1.0, p. 47, University of Kassel, Germany, 1997.

Alcamo, J., Flörke, M., and Märker, M.: Future long-term changes in global water resources driven by socio-economic and climatic changes, Hydrolog. Sci. J., 52, 247–275, doi:10.1623/hysj.52.2.247, 2007.

Amarasekera, K. N., Lee, R. F., Williams, E. R., and Eltahir, E. A. B.: ENSO and the natural variability in the flow of tropical rivers, J. Hydrol., 200, 24–39, 1997.

Arnell, N. W.: Effects of IPCC SRES* emissions scenarios on river runoff: a global perspective, Hydrol. Earth Syst. Sci., 7, 619–641, doi:10.5194/hess-7-619-2003, 2003.

Bouma, M. J., Kovats, R. S., Goubet, S. A., Cox, J. S. H., and Haines, A. T.: Global assessment of El Niño ’ s disaster burden, Lancet, 350, 1435–1438, 1997.

Bouwer, L. M., Vermaat, J. E., and Aerts, J. C. J. H.: Regional sensitivities of mean and peak river discharge to climate variability in Europe, J. Geophys. Res., 113, D19103, doi:10.1029/2008JD010301, 2008.

Cai, W., Borlace, S., Lengaigne, M., van Rensch, P., Collins, M., Vecchi, G., Timmermann, A., Santoso, A., McPhaden, M. J., Wu, L., England, M. H., Wang, G., Guilyardi, E., and Jin, F.-F.: Increasing frequency of extreme El Niño events due to greenhouse warming, Nature Climate Change, 4, 111–116, doi:10.1038/nclimate2100, 2014.

Cai, X. M. and Rosegrant, M. W.: Global Water Demand and Supply Projections, Water Int., 27, 159–169, doi:10.1080/02508060208686989, 2002.

Cheng, Y., Tang, Y., and Chen, D.: Relationship between predictability and forecast skill of ENSO on various time scales, J. Geophys. Res., 116, C12006, doi:10.1029/2011JC007249, 2011.

Chiew, F. H. S. and McMahon, T. A.: Global ENSO-streamflow teleconnection, streamflow forecasting and interannual variability, Hydrolog. Sci. J., 47, 505–522,doi:10.1080/02626660209492950, 2002.

Chiew, F. H. S., Piechota, T. C., Dracup, J. A., and McMahon, T. A.: El Nino Southern Oscillation and Australian rainfall, streamflow and drought: links and potential for forecasting, J. Hydrol., 204, 138–149, doi:10.1016/S0022-1694(97)00121-2 1998.

Chiew, F. H. S., Young, W. J., Cai, W., and Teng, J.: Current drought and future hydroclimate projections in southeast Australia and implications for water resources management, Stoch. Env. Res. Risk A, 25, 601–612, doi:10.1007/s00477-010-0424-x, 2011.

Clark II, C., Nnaji, G. A., and Huang, W.: Effects of f El-Niño and a La-Niña Sea Surface Temperature Anomalies on Annual Precipitations and Streamflow Discharges in Southeastern United States, J. Coastal Res., 68, 113–120, doi:10.2112/SI68-015.1, 2014.

Coughlan de Perez, E., Monasso, F., van Aalst, M., and Suarez, P.: Science to prevent disasters, Nat. Geosci., 7, 78–79, doi:10.1038/ngeo2081, 2014a.

Coughlan de Perez, E., van den Hurk, B., van Aalst, M. K., Jongman, B., Klose, T., and Suarez, P.: Forecast-based financing: an approach for catalyzing humanitarian action based on extreme weather and climate forecasts, Nat. Hazards Earth Syst. Sci., 15, 895–904, doi:10.5194/nhess-15-895-2015, 2015.

De Fraiture, C.: Integrated water and food analysis at the global and basin level, an application of WATERSIM, Water Resour. Manag., 21, 185–198, doi:10.1007/s11269-006-9048-9, 2007.

Dettinger, M. D. and Diaz, H. F.: Global characteristics of stream flow seasonality and variability, J. Hydrometeorol., 1, 289–310, 2000.

Dettinger, M. D., Cayan, D. R., Mccabe, G. J., and Marengo, J. A.: Multiscale streamflow variability associated with El Niño/Southern Oscillation, in: El Nino and the Southern Oscillation – Multiscale Variability and Global and Regional Impacts, edited by: Diaz, H. F. and Markgraf, V., El Niño and the Southern Oscillation–Multiscale Variability and Global and Regional Impacts, Cambridge University Press, 113–146, 2000.

Dilley, M.: Reducing vulnerability to climate variability in Southern Africa: the growing role of climate information, Climatic Change, 45, 63–73, 2000.

Title Page
Abstract | Introduction
Conclusions | References
Tables | Figures
◂◂ | ▸▸
◂ | ▸
Back | Close
Full Screen / Esc
Printer-friendly Version
Interactive Discussion

Dilley, M. and Heyman, B. N.: ENSO and disaster: droughts, floods and El Nino/Southern Oscillation warm events, Disasters, 19, 181–193, 1995.

Döll, P. and Lehner, B.: Validation of a new global 30-min drainage direction map, J. Hydrol., 258, 214–231, 2002.

Dutta, S. C., Ritchie, J. W., Freebairn, D. M., and Abawi, G. Y.: Rainfall and streamflow response to El Niño Southern Oscillation: a case study in a semiarid catchment, Australia, Hydrolog. Sci. J., 51, 1006–1020, doi:10.1623/hysj.51.6.1006, 2006.

Falkenmark, M.: Fresh water – time for a modified approach, Ambio, 15, 192–200, 1986.

Falkenmark, M.: Growing water scarcity in agriculture?: future challenge to global water security, Philos. T. Roy. Soc. A, 371, 20120410, doi:10.1098/rsta.2012.0410, 2013.

Gerten, D., Heinke, J., Hoff, H., Biemans, H., Fader, M., and Waha, K.: Global water availability and requirements for future food production, J. Hydrometeorol., 12, 885–899, doi:10.1175/2011JHM1328.1, 2011.

Guilyardi, E., Wittenberg, A., Fedorov, A., Collins, M., Wang, C., Capotondi, A., van Oldenborgh, G. J., and Stockdale, T.: Understanding El Niño in ocean–atmosphere general circulation models, progress and challenges, B. Am. Meteorol. Soc., 90, 325–340, 2009.

Grey, D. and Sadoff, C. W.: Sink or swim? Water security for growth and development, Water Policy, 9, 545, doi:10.2166/wp.2007.021, 2007.

Gudmundsson, L., Wagener, T., Tallaksen, L. M., and Engeland, K.: Evaluation of nine large-scale hydrological models with respect to the seasonal runoff climatology in Europe, Water Resour. Res., 48, W11504, doi:10.1029/2011WR010911, 2012.

Haddeland, I., Heinke, J., Voß, F., Eisner, S., Chen, C., Hagemann, S., and Ludwig, F.: Effects of climate model radiation, humidity and wind estimates on hydrological simulations, Hydrol. Earth Syst. Sci., 16, 305–318, doi:10.5194/hess-16-305-2012, 2012.

Haddeland, I., Heinke, J., Biemans, H., Eisner, S., Flörke, M., Hanasaki, N., Konzmann, M., Ludwig, F., Masaki, Y., Schewe, J., Stacke, T., Tessler, Z. D., Wada, Y., and Wisser, D.: Global water resources affected by human interventions and climate change, P. Natl. Acad. Sci. USA, 111, 3251– 3256 doi:10.1073/pnas.1222475110, 2014.

Hall, J. and Borgomeo, E.: Risk-based principles for defining and managing water security Risk-based principles for defining and managing water security, Philos. T. Roy. Soc. A, 371, 20120407, doi:10.1098/rsta.2012.0407, 2013.

Hanemann, W. M.: The economic conception of water, in: Water Crisis: Myth or Reality?, edited by: Rogers, P. R., Ramon Llamas, M., Martinez-Cortina, L., Taylor & Francis/Balkema, Leiden, The Netherlands, 61–90, 2006.

Hannah, D. M., Demuth, S., van Lanen, H. A. J., Looser, U., Prudhomme, C., Rees, G., Stahl, K., and Tallaksen, L. M.: Large-scale river flow archives: importance, current status and future needs, Hydrol. Process., 25, 1191–1200, doi:10.1002/hyp.7794, 2011.

Hoekstra, A. Y., Mekonnen, M. M., Chapagain, A. K., Mathews, R. E., and Richter, B. D.: Global monthly water scarcity: blue water footprints versus blue water availability, PloS One, 72, e32688, doi:10.1371/journal.pone.0032688, 2012.

Howell, L.: Global Risks, World Economic Forum, Geneva, Switzerland, 2013.

Hulme, M., Barrow, E. M., Arnell, N. W., Harrison, P. A., and Johns, T. C.: Relative impacts of human-induced climate change and natural climate variability, Nature, 3976721, 688–691, 1999.

IPCC.: Summary for Policymakers. Climate Change 2013: The Physical Science Basis, Contribution of Working Group I to the Fifth Assessment Report of the Intergovernmental Panel on Climate Change, Cambridge Univ. Press, Cambridge, UK, 2013.

Kiem, A. S. and Franks, S. W.: On the identification of ENSO-induced rainfall and runoff variability: a comparison of methods and indices, Hydrolog. Sci. J., 46, 715–727, doi:10.1080/02626660109492866, 2001.

Kiguchi, M., Shen, Y., Kanae, S., and Oki, T.: Reevaluation of future water stress due to socio-economic and climate factors under a warming climate, Hydrolog. Sci. J., 60, 14–29, doi:10.1080/02626667.2014.888067, 2014.

Kiladis, G. N. and Diaz, H. F.: Global climatic anomalies associated with extremes in the Southern Oscillation, J. Climate, 2, 1069–1090, 1989.

Klein Goldewijk, K. and van Drecht, G.: HYDE 3: Current and historical population and land cover. MNP 2006, in: Integrated Modelling of Global Environmental Change. An Overview of IMAGE 2.4, edited by: Bouwman, A. F., Kram, T., and Klein Goldewijk, K., Netherlands Environmental Assessment Agency (MNP), Bilthoven, 2006.

Kovats, R. S., Bouma, M. J., Hajat, S., Worrall, E., and Haines, A.: El Niño and Health, The Lancet, 362, 1481–1489, 2003.

Kummu, M., Ward, P. J., de Moel, H., and Varis, O.: Is physical water scarcity a new phenomenon? Global assessment of water shortage over the last two millennia, Environ. Res. Lett., 5, 034006, doi:10.1088/1748-9326/5/3/034006, 2010.

Kummu, M., Gerten, D., Heinke, J., Konzmann, M., and Varis, O.: Climate-driven interannual variability of water scarcity in food production potential: a global analysis, Hydrol. Earth Syst. Sci., 18, 447–461, doi:10.5194/hess-18-447-2014, 2014.

Labat, D.: Cross wavelet analyses of annual continental freshwater discharge and selected climate indices, J. Hydrol., 385, 269–278, doi:10.1016/j.jhydrol.2010.02.029, 2010.

Lehner, B., Döll, P., Alcamo, J., Henrichs, T., and Kaspar, F.: Estimating the impact of global change on flood and drought risks in Europe: a continental, integrated analysis, Climatic Change, 75, 273–299, doi:10.1007/s10584-006-6338-4, 2006.

Livezey, R. E. and Chen, W. Y.: Statistical field significance and its determination by monte carlo techniques, Mon. Weather Rev., 111, 46–59, 1982.

Lü, A., Jia, S., Zhu, W., Yan, H., Duan, S., and Yao, Z.: El Niño-Southern Oscillation and water resources in the headwaters region of the Yellow River: links and potential for forecasting, Hydrol. Earth Syst. Sci., 15, 1273–1281, doi:10.5194/hess-15-1273-2011, 2011.

Ludescher, J., Gozolchiani, A., Bogachev, M. I., Bunde, A., Havlin, S., and Schellnhuber, H. J.: Improved El Nino forecasting by cooperativity detection, P. Natl. Acad. Sci. USA, 110, 19172–19173, doi:10.1073/pnas.1317354110, 2013.

Ludescher, J., Gozolchiani, A., Bogachev, M. I., Bunde, A., Havlin, S., Schellnhuber, H. J.: Very early warning of next El Niño, P. Natl. Acad. Sci. USA, 111, 2064–2066, 2014.

Lundqvist, J. and Falkenmark, M.: Adaptation to rainfall variability and unpredictability: new dimensions of old challenges and opportunities, Int. J. Water Resour. D, 26, 595–612, doi:10.1080/07900627.2010.519488, 2010.

McPhaden, M. J., Zebiak, S. E., and Glantz, M. H.: ENSO as an integrating concept in earth science, Science, 314, 1740–1745, doi:10.1126/science.1132588, 2006.

Meque, A. and Abiodun, B. J.: Simulating the link between ENSO and summer drought in Southern Africa using regional climate models, Clim. Dynam., 44, 1881–1900, doi:10.1007/s00382-014-2143-3, 2014.

Mosley, M. P.: Regional differences in the effects of El Niño and La Niña on low flows and floods, Hydrolog. Sci. J., 45, 249–267, doi:10.1080/02626660009492323, 2000.

Moss, M. E., Pearson, C. P., and McKerchar, A. I.: The Southern Oscillation index as a predictor of the probability of low streamflows in New Zealand, Water Resour. Res., 30, 2717–2723, 1994.

Murphy, J., Kattsov, V., Keenlyside, N., Kimoto, M., Meehl, G., Mehta, V., Pohlman, H., Scaife, A., and Smith, D.: Towards prediction of decadal climate variability and change procedia environmental sciences, Procedia Environmental Sciences, 1, 287–304, doi:10.1016/j.proenv.2010.09.018, 2010.

Nazemi, A. and Wheater, H. S.: On inclusion of water resource management in Earth system models – Part 1: Problem definition and representation of water demand, Hydrol. Earth Syst. Sci., 19, 33–61, doi:10.5194/hess-19-33-2015, 2015a.

Nazemi, A. and Wheater, H. S.: On inclusion of water resource management in Earth system models – Part 2: Representation of water supply and allocation and opportunities for improved modeling, Hydrol. Earth Syst. Sci., 19, 63–90, doi:10.5194/hess-19-63-2015, 2015b.

Oki, T. and Kanae, S.: Global hydrological cycles and world water resources, Science, 3135790, 1068–72, doi:10.1126/science.1128845, 2006.

Paeth, H., Scholten, A., Friederichs, P., Hense, A.: Uncertainties in climate change prediction: El Niño Southern Oscillation and monsoons, Global Planet Change, 60, 265–288, 2008.

Parker, D., Folland, C., Scaife, A., Knight, J., Colman, A., Baines, P., and Dong, B.: Decadal to multidecadal variability and the climate change background, J. Geophys. Res., 112, D18115, doi:10.1029/2007JD008411, 2007.

Piechota, T. C. and Dracup, J. A.: Long-range forecasting using El-Nino Southern Oscillations indicators, J. Hydrol. Eng., 4, 144–151, 1999.

Power, S., Delage, F., Chung, C., Kociuba, G., and Keay, K.: Robust twenty-first-century projections of El Niño and related precipitation variability, Nature, 5027472, 541–545 doi:10.1038/nature12580, 2013.

Prudhomme, C., Giuntoli, I., Robinson, E. L., Clark, D. B., Arnell, N. W., Dankers, R., Fekete, B. M., Franssen, W., Gerten, D., Gosling, S. N., Hagemann, S., Hannah, D. M., Kim, H., Masaki, Y., Satoh, Y., Stacke, T., Wada, Y., and Wisser, D.: Hydrological droughts in the 21st century, hotspots and uncertainties from a global multimodel ensemble experiment, P. Natl. Acad. Sci. USA, 111, 3262– 3267 doi:10.1073/pnas.1222473110, 2014.

Räsänen, T. A. and Kummu, M.: Spatiotemporal influences of ENSO on precipitation and flood pulse in the Mekong River Basin, J. Hydrol., 476, 154–168, doi:10.1016/j.jhydrol.2012.10.028, 2013.

Richard, Y., Fauchereau, N., Poccard, I., Rouault, M., and Trzaska, S.: 20th century droughts in Southern Africa: spatial and temporal variability, teleconnections with oceanic and atmospheric conditions, Int. J. Climatol., 21, 873–885, doi:10.1002/joc.656, 2001.

Rijsberman, F.: Water scarcity: fact or fiction? Agr. Water Manage., 80, 5–22, doi:10.1016/j.agwat.2005.07.001, 2006.

Rosegrant, M. W., Cai, X. M., and Cline, S.: World Water and Food to 2025. Dealing with Scarcity, International Food Policy Research Institute, Washington, D.C., 2002.

Rosenzweig, C. and Hillel, D.: Climate Variability and the Global Harvest: Impacts of El Nino and Other Oscillations on Agro-Ecosystems, p. 280, Oxford University Press, New York, 2008.

Schewe, J., Heinke, J., Gerten, D., Haddeland, I., Arnell, N. W., Clark, D. B., Dankers, R., Eisner, S., Fekete, B. M., Colón-González, F. J., Gossling, S. N., Kim, H., Liu, X., Masaki, Y., Portmann, F. T., Satoh, Y., Stacke, T., Tang, Q., Wada, Y., Wisser, D., Albrecht, T., Frieler, K., Piontek, F., Warszawski, L., and Kabat, P.: Multimodel assessment of water scarcity under climate change, P. Natl. Acad. Sci. USA, 111, 3245–3250, doi:10.1073/pnas.1222460110, 2014.

Schmidt, N., Lipp, E. K., Rose, J. B., and Luther, M. E.: ENSO influences on seasonal rainfall and river discharge in Florida, J. Climate, 14, 615–628, 2001.

Sheffield, J., Andreadis, K. M., Wood, E. F., Lettenmaier, D. P.: Global and continental drought in the second half of the twentieth century: severity-area-duration analysis and temporal variability of large-scale events, J. Climate, 22, 1962–1981, doi:10.1175/2008JCLI2722.1, 2008.

Smit, B. and Pilifosova, O.: From adaptation to adaptive capacity and vulnerability reduction, in: Climate Change, Adaptive Capacity and Development, edited by: Smith, J. B., Klein, R. J. T., and Huq, S., Imperial College Press, London, 2003.

Sharma, A.: Seasonal to interannual rainfall probabilistic forecasts for improved water supply management?: Part 3 – A nonparametric probabilistic forecast model, J. Hydrol., 239, 249–258, 2000.

Sperna Weiland, F. C., van Beek, L. P. H., Kwadijk, J. C. J., and Bierkens, M. F. P.: Global patterns of change in discharge regimes for 2100, Hydrol. Earth Syst. Sci., 16, 1047–1062, doi:10.5194/hess-16-1047-2012, 2012.

Stahl, K.: Hydrological Drought – a Study across Europe, PhD thesis, Freiburger Schriften zur hydrologie (No. 15), Institut fur Hydrologies, Universitat Freiburg, Freiburg, 2001.

Suarez, P., Hansen, J. W., Carriquiry, M., Mishra, A. K., and Osgood, D.: Integrating seasonal forecasts and insurance for adaptation among subsistence farmers: The case of Malawi (No. 4651), World Bank Policy Research Working Paper series, available at SSRN: http://ssrn.com/abstract=1149603, last access: 5 May 2015, 2008.

Van Beek, L. P. H., Wada, Y., and Bierkens, M. F. P.: Global monthly water stress: 1. Water balance and water availability, Water Resour. Res., 47, W07517, doi:10.1029/2010WR009791, 2011.

van Oldenborgh, G. J., Philip, S. Y., and Collins, M: El Niño in a changing climate: a multi-model study, Ocean Sci., 1, 81–95, doi:10.5194/os-1-81-2005, 2005.

Van Vliet, M. T. H., Franssen, W. H. P., Yearsley, J. R., Ludwig, F., Haddeland, I., Lettenmaier, D. P., and Kabat, P.: Global river discharge and water temperature under climate change, Global Environ. Chang., 23, 450–464, doi:10.1016/j.gloenvcha.2012.11.002, 2013.

Veldkamp, T. I. E., Wada, Y., de Moel, H., Kummu, M., Eisner, S., Aerts, J. C. J. H., and Ward, P. J.: Changing mechanism of global water scarcity events: impacts of socioeconomic changes and inter-annual hydro-climatic variability, Global Environ. Chang., 32, 18–29, doi:10.1016/j.gloenvcha.2015.02.011, 2015.

Vorosmarty, C. J., Green, P., Salisbury, J., and Lammers, R. B.: Global water resources: vulnerability from climate change and population growth, Science, 289, 284–288, doi:10.1126/science.289.5477.284, 2000.

Wada, Y., van Beek, L. P. H., and Bierkens, M. F. P.: Modelling global water stress of the recent past: on the relative importance of trends in water demand and climate variability, Hydrol. Earth Syst. Sci., 15, 3785–3808, doi:10.5194/hess-15-3785-2011, 2011a.

Wada, Y., van Beek, L. P. H., Viviroli, D., Dürr, H. H., Weingartner, R., and Bierkens, M. F. P.: Global monthly water stress: 2. Water demand and severity of water stress, Water Resour. Res., 47, W07518, doi:10.1029/2010WR009792, 2011b.

Wada, Y., Gleeson, T., and Esnault, L.: Water wedges?: Regional strategies to global water resource wedge approach to water stress, Nat. Geosci., 7, 615–617, doi:10.1038/NGEO2241, 2014a.

Wada, Y., Wisser, D., and Bierkens, M. F. P.: Global modeling of withdrawal, allocation and consumptive use of surface water and groundwater resources, Earth Syst. Dynam., 5, 15–40, doi:10.5194/esd-5-15-2014, 2014b.

Wallace, J. M. and Hobbs, P.: Atmospheric Science, 2nd edn., p. 504, Academic Press, 2006.

Wang, C., Xie, S., and Carton, J. A.: A global survey of ocean–atmosphere interaction and climate variability, in: Earth Climate: The Ocean–Atmospheric Interaction, edited by: Wang, C., Xie, S. P., and Carton, J. A., Publisher & Publishing location: American Geophysical Union, Washington, D.C., 1–19, doi:10.1029/147GM01, 2004.

Ward, P. J., Aerts, J. C. J. H., de Moel, H., and Renssen, H.: Verification of a coupled climate-hydrological model against Holocene palaeohydrological records, Global Planet. Change, 57, 283–300, doi:10.1016/j.gloplacha.2006.12.002, 2007.

Ward, P. J., Beets, W., Bouwer, L. M., Aerts, J. C. J. H., and Renssen, H.: Sensitivity of river discharge to ENSO, Geophys. Res. Lett., 37, L12402, doi:10.1029/2010GL043215, 2010.

Ward, P. J., Eisner, S., Flörke, M., Dettinger, M. D., and Kummu, M.: Annual flood sensitivities to El Niño–Southern Oscillation at the global scale, Hydrol. Earth Syst. Sci., 18, 47–66, doi:10.5194/hess-18-47-2014, 2014.

Ward, P. J., Jongman, B., Kummu, M., Dettinger, M. D., Sperna Weiland, F. C., and Winsemius, H. C.: Strong influence of El Nino Southern Oscillation on flood risk around the world, P. Natl. Acad. Sci. USA, 111, 15659–15664, doi:10.1073/pnas.1409822111, 2014b.

Weedon, G. P., Gomes, S., Viterbo, P., Shuttleworth, W. J., Blyth, E., Österle, H., Adam, J. C., Bellouin, N., Boucher, O., and Best, M.: Creation of the watch forcing data and its use to assess global and regional reference crop evaporation over land during the twentieth century, J. Hydrometeorol., 12, 823–848, doi:10.1175/2011JHM1369.1, 2011.

Weedon, G. P., Balsamo, G., Bellouin, N., Gomes, S., Best, M. J., and Viterbo, P.: The WFDEI meteorological forcing data set: WATCH forcing data methodology applied to ERA-interim reanalysis data, Water Resour. Res., 50, 7505–7514, doi:10.1002/2014WR015638, 2014.

Whetton, P. H., Adamson, D. A., and Wilson, M. A. J.: Rainfall and River Flow Variability in Africa, Australia and East Asia linked to El Nino –Southern Oscillation events, in: Lessons for Human Survival: Nature's record from the Quaternary, edited by: Bishop, P., Geological Society of Australia Symposium Proceedings, 1, 71–82, 1990.

Young, R. A.: Determining the Economic Value of Water: Concepts and Methods, Resources for the Future, Washington D.C., USA, p. 357, 2005.

Zebiak, S. E., Orlove, B., Muñoz, Á. G., Vaughan, C., Hansen, J., Troy, T., Thomson, M. C., Lustig, A., and Garvin, S.: Investigating El Niño–Southern Oscillation and society relationships, Wiley Interdisciplinary Reviews: Clim. Change, 6, 17–34, doi:10.1002/wcc.294, 2014.

Table 1. Hydrological years that fall under the El Niño and La Niña phase. Other years are classified as ENSO neutral.

ENSO phase	Hydrological year
El Niño	1964, 1966, 1970, 1973, 1977, 1983, 1987, 1988, 1992, 1998, 2003, 2007, 2010
La Niña	1965, 1968, 1971, 1972, 1974, 1975, 1976, 1989, 1999, 2000, 2008

(a) Water availability

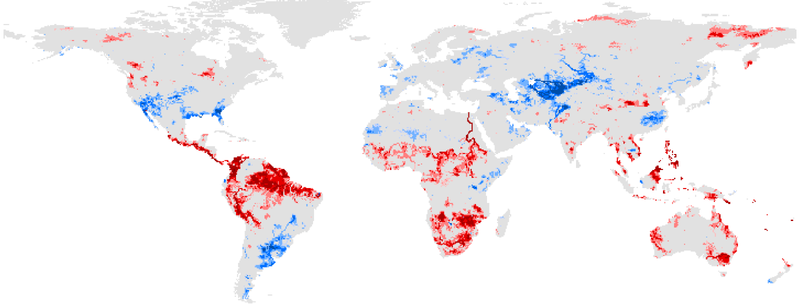

(b) Consumptive water use

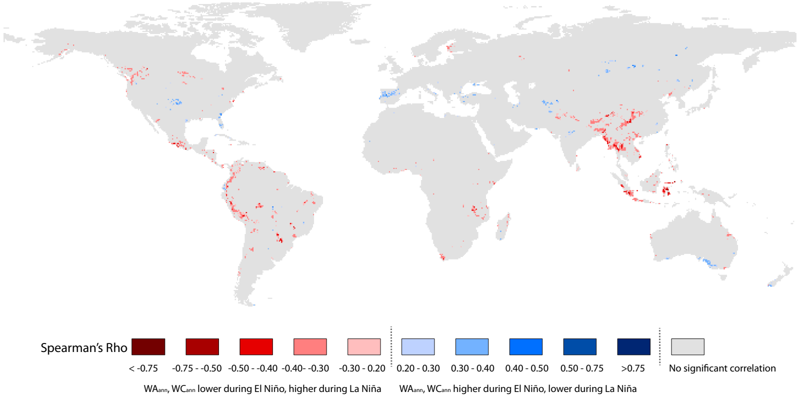

Figure 1. Correlation (Spearman's Rho) of yearly **(a)** water availability and **(b)** consumptive water use values to variations in JMA $\mathrm{SST}_{\mathrm{bestoff}}$. Significance was tested by means of regular bootstrapping ($n = 1000$, $p = 0.05$) and the correlation is only shown for those areas which reach significance. Positive correlations indicate increases in annual water availability and consumption with the JMA $\mathrm{SST}_{\mathrm{bestoff}}$ index moving towards El Niño values. Negative correlations indicate decreases in annual water availability with the JMA $\mathrm{SST}_{\mathrm{bestoff}}$ index moving towards El Niño values.

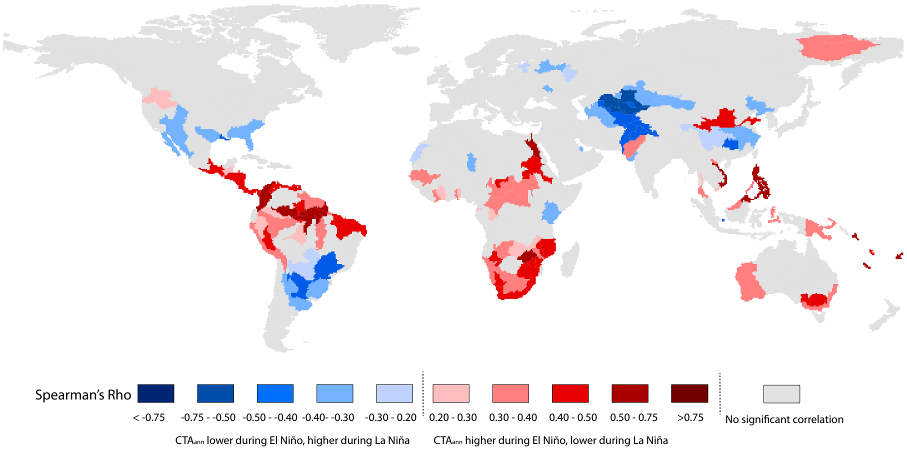

Figure 2. Correlation (Spearman's Rho) of yearly water scarcity conditions (CTA-ratio) to variations in JMA $\text{SST}_{\text{bestoff}}$. Significance was tested by regular bootstrapping ($n = 1000$, $p = 0.05$) and the correlation is only shown for those areas with significant correlations. Positive correlations indicate increases in CTA-ratio values (more severe water scarcity conditions) with the JMA $\text{SST}_{\text{bestoff}}$ index moving towards El Niño values. Negative correlations indicate decreases in CTA-ratio values (less severe water scarcity conditions) with the JMA $\text{SST}_{\text{bestoff}}$ index moving towards El Niño values.

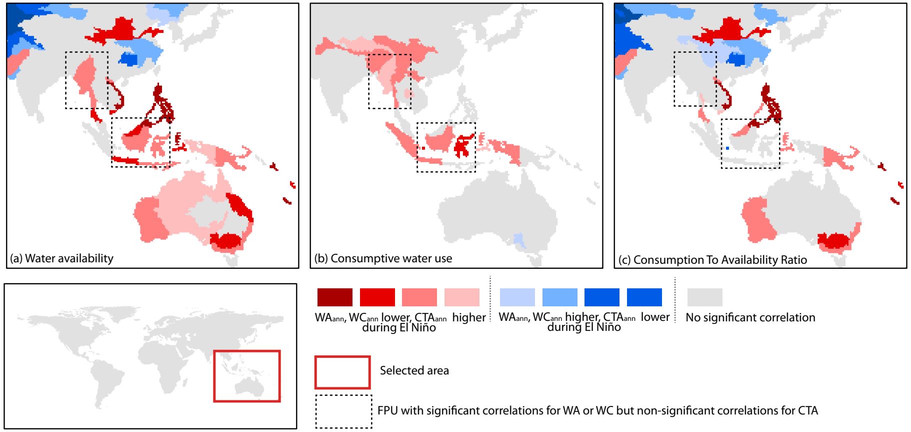

Figure 3. Correlation (Spearman's Rho) of yearly **(a)** water availability; **(b)** water consumption values; and **(c)** water scarcity conditions (CTA-ratio) to variation in JMA $\text{SST}_{\text{bestoff}}$ for a selected area. Significance was tested by regular bootstrapping ($n = 1000$, $p = 0.05$) and the correlation is only shown for those areas with significant correlations. Comparison of the results found in **(a, b)**, and **(c)** indicate significant correlations for water availability and water consumption, but no significant correlations when considering water scarcity conditions (CTA-ratio).

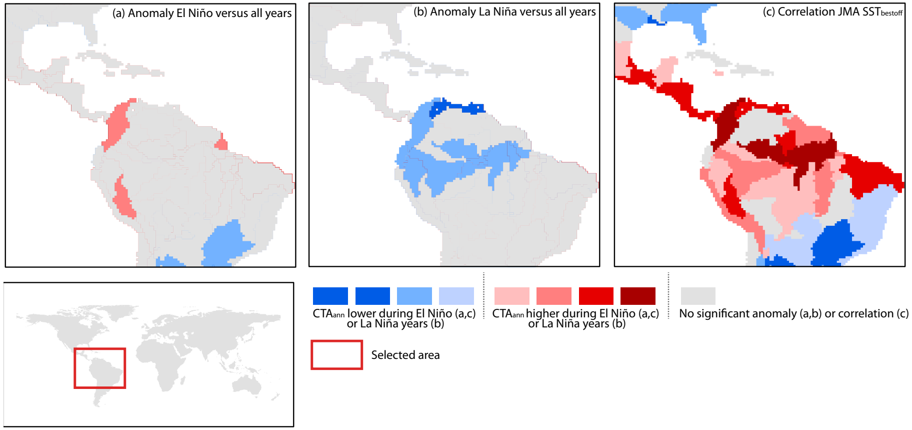

Figure 4. Comparison of significance of results found when studying the: **(a)** anomaly in water scarcity conditions (CTA-ratio) between El Niño and all years; **(b)** anomaly in water scarcity conditions (CTA-ratio) between La Niña and all years; and **(c)** the sensitivity of water scarcity conditions (CTA-ratio) to ENSO driven climate variability measured by means of the JMA SST$_{bestoff.}$ Red colors indicate more severe scarcity conditions under El Niño phases **(a, c)** or La Niña phases **(b)**. Blue colors indicate less severe scarcity conditions under El Niño phases **(a, c)** or La Niña phases **(b)**.

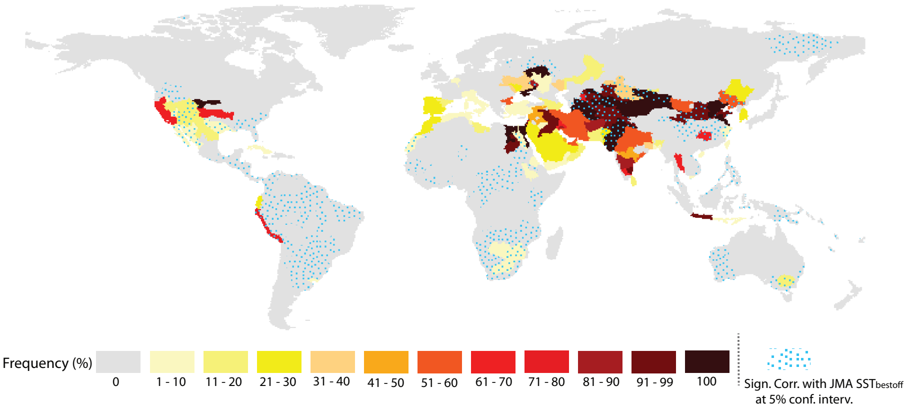

Figure 5. Frequency (%) of water scarcity events (CTA-ratio) over the period 1961–2010. The dots indicate whether the water scarcity conditions in a FPU could be significantly correlated to variation to JMA SST$_{\text{bestoff}}$ at a 5 % confidence interval (tested using regular bootstrapping, $n = 1000$).

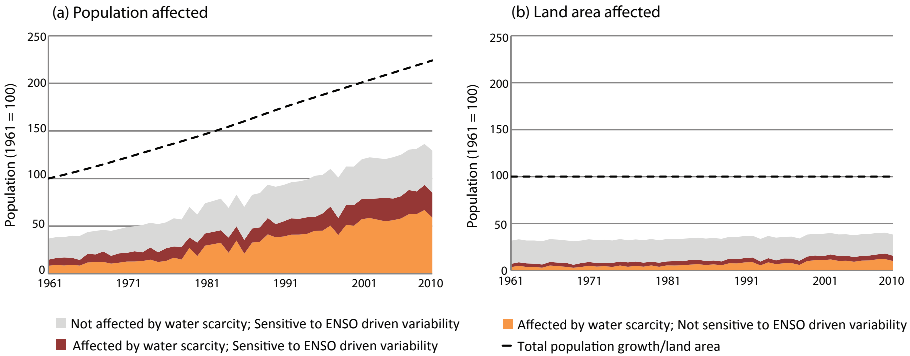

Figure 6. Increase in population and land area affected by either water scarcity events and/or ENSO driven climate variability over the period 1961–2010, as estimated with the CTA-ratio. **(a)** shows the growth in population living under water scarce conditions and/or living in areas sensitive to ENSO driven climate variability relative to the total growth in global population (set at 100 in 1961). **(b)** shows the increase in land area affected by either water scarcity events and/or ENSO driven climate variability relative to the total global land area (100).

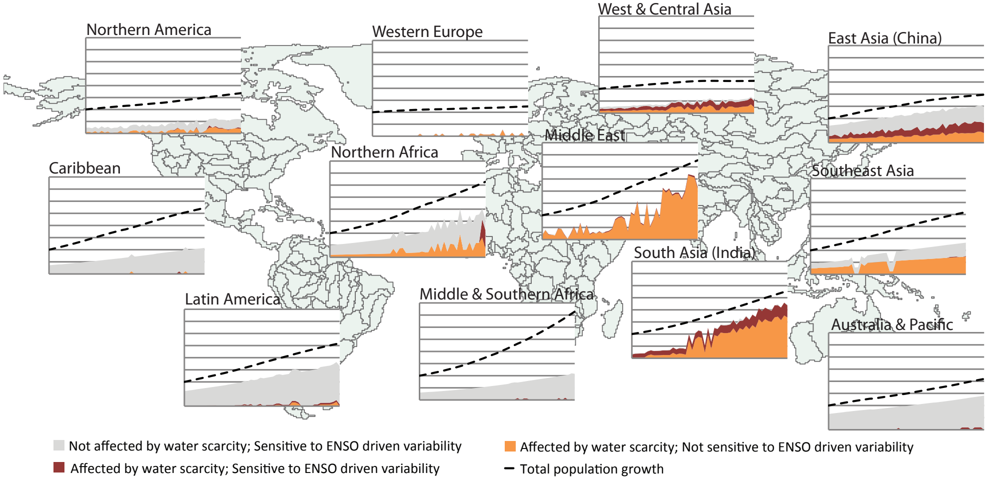

Figure 7. Regional variation in developments of population (%) affected by either water scarcity events and/or ENSO driven climate variability over the period 1961–2010, as estimated with the CTA-ratio. The figure shows per world region the growth in population living under water scarcity conditions and/or living in areas sensitive to ENSO riven climate variability, relative to the total growth in global population (set at 100 in 1961). *Y* axis (% population affected) ranges from 0 up to 400.

Title Page
Abstract Introduction
Conclusions References
Tables Figures
◂ ▸
Back Close
Full Screen / Esc
Printer-friendly Version
Interactive Discussion

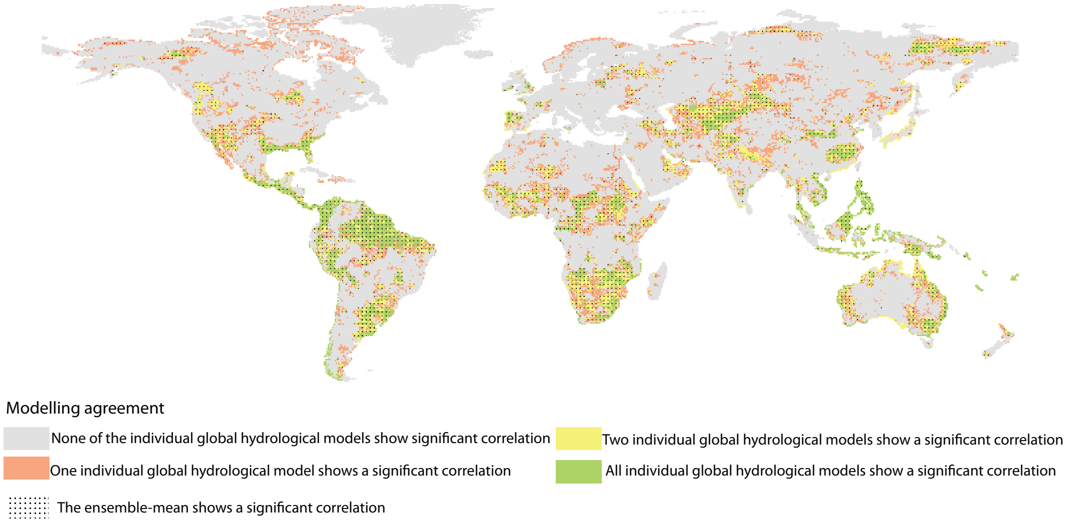

Figure 8. Modelling agreement in observed significant sensitivity of water availability to variation in JMA SST, measured at the grid-cell level.

(a) Consumption To Availability Ratio

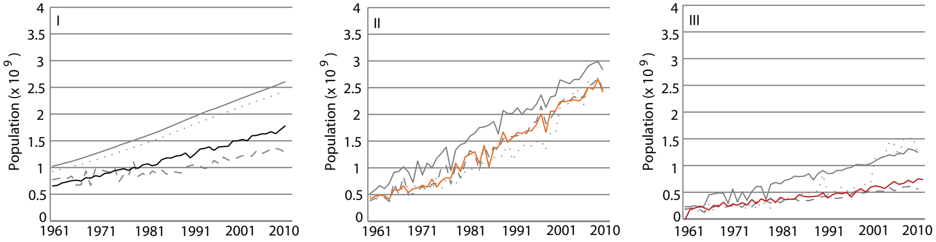

(b) Water Crowding Index

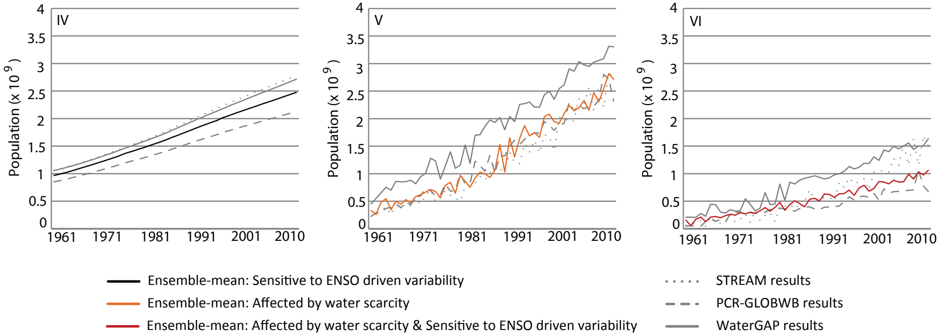

Figure 9. Developments in population sensitive to ENSO driven climate variability and/or affected by water scarcity events as assessed by the individual global hydrological models (STREAM, PCR-GLOBWB, and WaterGAP) and the ensemble-mean. Panels I and IV show the development in population to ENSO driven climate variability while panels II and V give the increase in population being affected by water scarcity events. Panels III and VI visualize the amount of people being affected by water scarcity events while at the same time living in areas with a significant correlation to ENSO driven climate variability.

(a) Pixel scale

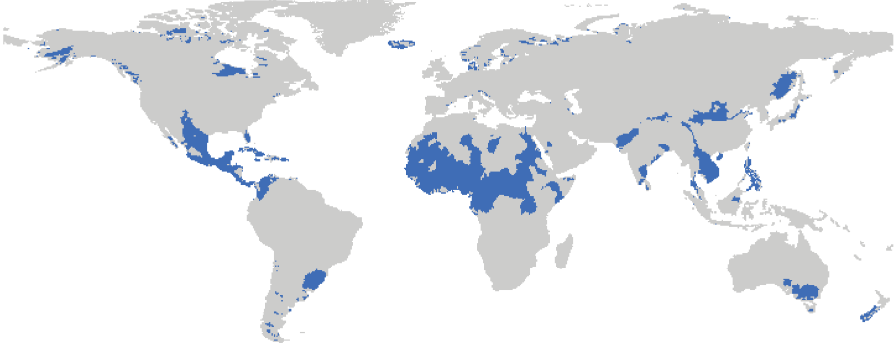

(b) FPU scale

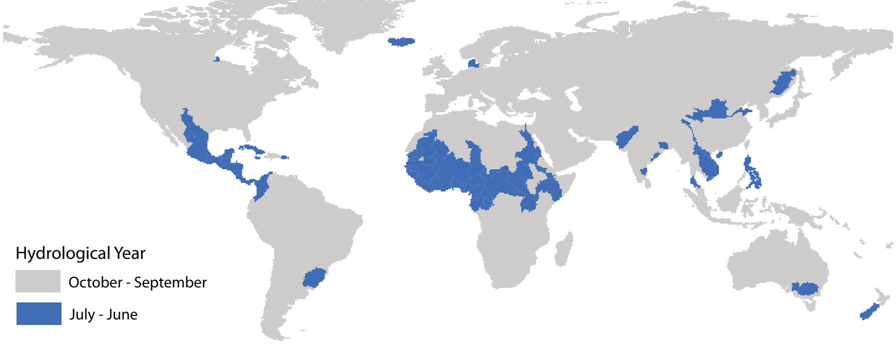

Figure A1. Hydrological years used in this study.

(a) Water availability

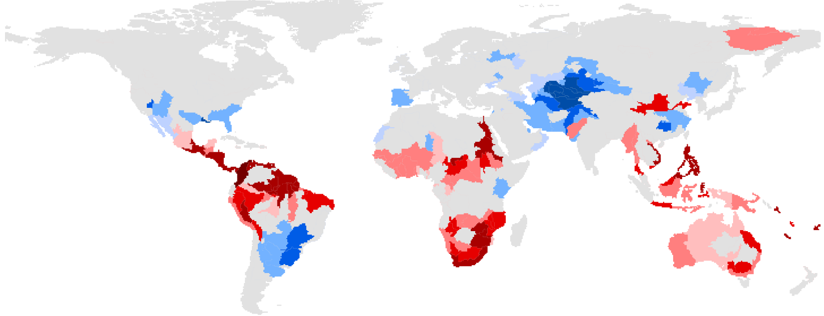

(b) Consumptive water use

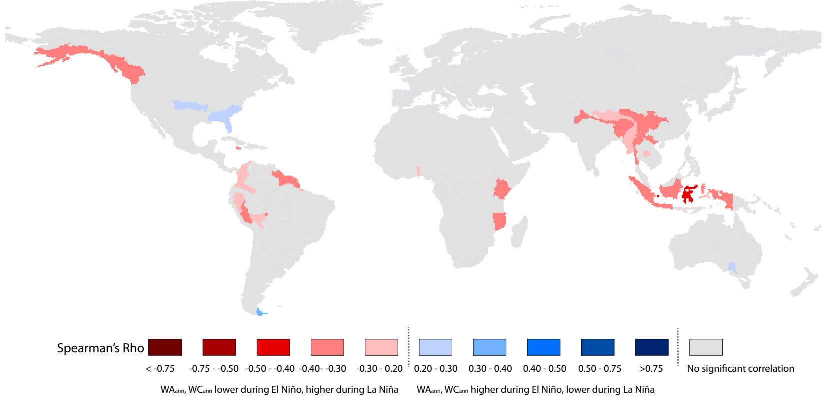

Figure A2. Correlation (Spearman's Rho) of yearly **(a)** water availability and **(b)** consumptive water use values to variations in JMA SST$_{\text{bestoff}}$. Significance was tested by regular bootstrapping ($n = 1000$, $\alpha = 0.05$) and the correlation is only shown for those areas with significant correlations. Positive correlations indicate increases in annual water availability and consumption with the JMA SST$_{\text{bestoff}}$ index moving towards El Niño values. Negative correlations indicate decreases in annual water availability with the JMA SST$_{\text{bestoff}}$ index moving towards El Niño values.

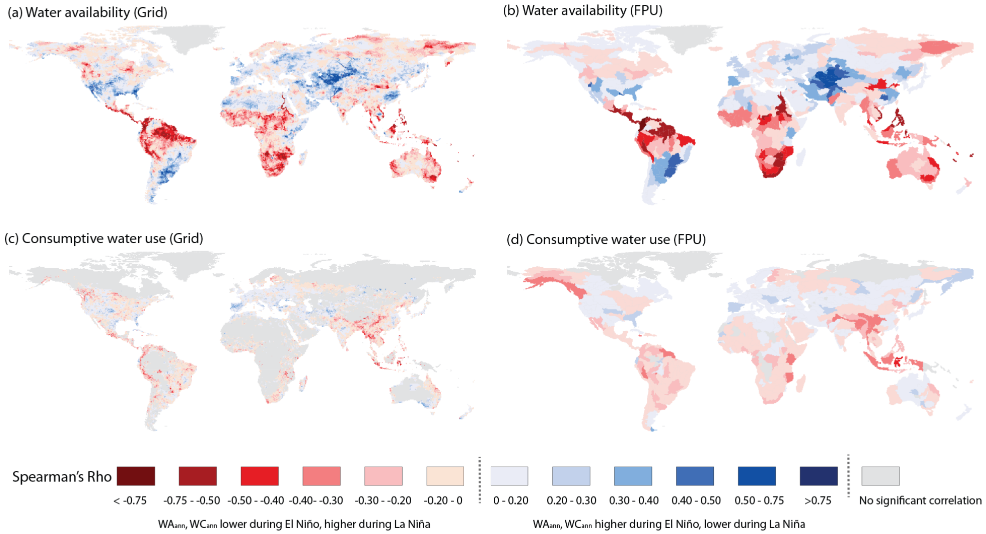

Figure A3. Correlation (Spearman's Rho) of yearly **(a–b)** water availability and **(c–d)** consumptive water use values to variations in JMA SST$_{\text{bestoff}}$. Positive correlations indicate increases in annual water availability and consumption with the JMA SST$_{\text{bestoff}}$ index moving towards El Niño values. Negative correlations indicate decreases in annual water availability with the JMA SST$_{\text{bestoff}}$ index moving towards El Niño values.

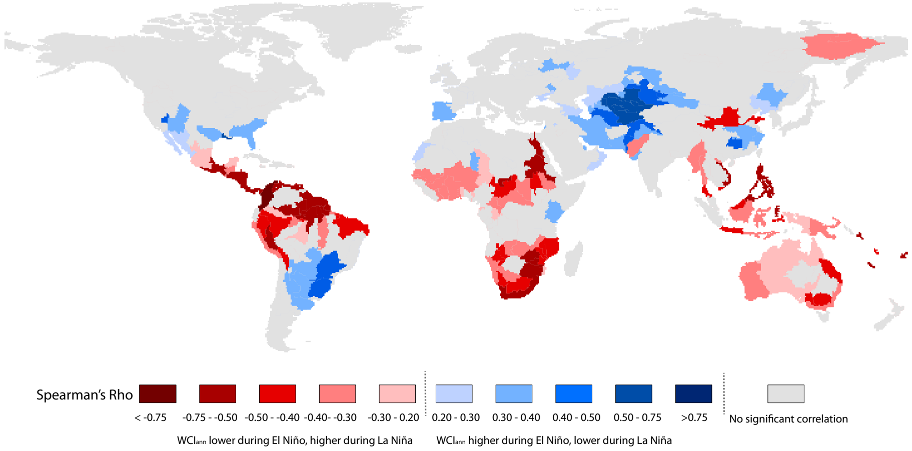

Figure A4. Correlation (Spearman's Rho) of yearly water shortage conditions (WCI) to variations in JMA SST$_{\text{bestoff}}$. Significance was tested by regular bootstrapping ($n = 1000$, $\alpha = 0.05$) and the correlation is only shown for those areas with significant correlations. Positive correlations indicate increases in WCI values (less severe water scarcity conditions) with the JMA SST$_{\text{bestoff}}$ index moving towards El Niño values. Negative correlations indicate decreases in WCI values (more severe water scarcity conditions) with the JMA SST$_{\text{bestoff}}$ index moving towards El Niño values.

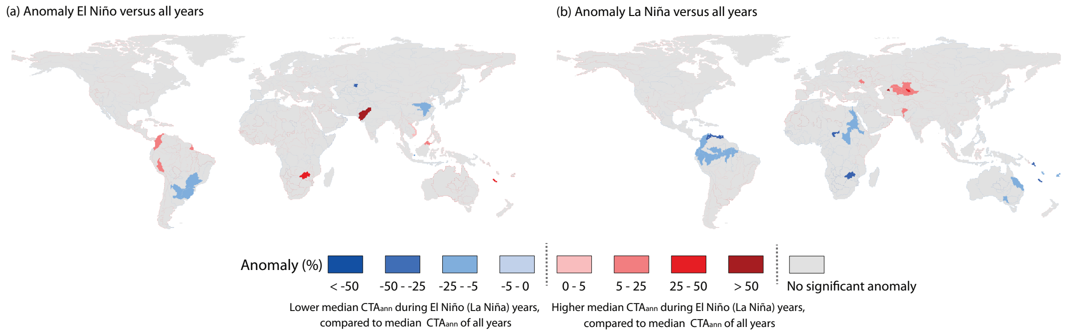

(a) Anomaly El Niño versus all years

(b) Anomaly La Niña versus all years

Figure A5. Percentage anomaly per FPU in water stress conditions measured by the CTA-ratio for: (I) El Niño years compared to all years, and (II) La Niña year compared to all years. Statistical significance was tested with a bootstrapped MWU-test ($n = 1000$, $\alpha = 0.05$). Positive values show higher than average (all years) median CTA-ratio values indicating more severe water stress conditions whereas negative values show lower than average (all years) median CTA-ratio values indicating less severe water stress conditions.

Title Page
Abstract
Introduction
Conclusions
References
Tables
Figures
◀|
|▶
◀
▶
Back
Close
Full Screen / Esc
Printer-friendly Version
Interactive Discussion

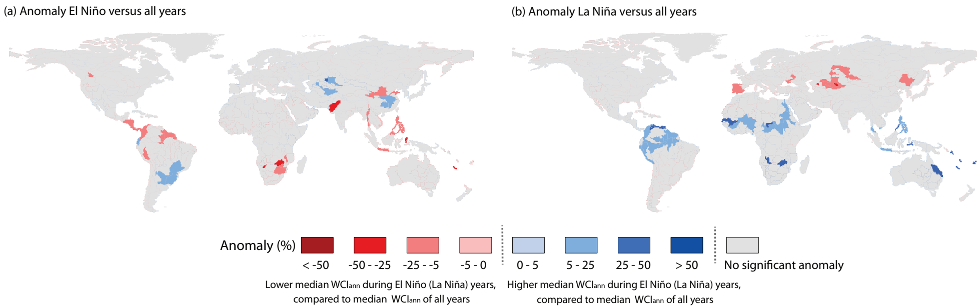

Figure A6. Percentage anomaly per FPU in water shortage conditions measured by the WCI for: (I) El Niño years compared to all years, and (II) La Niña year compared to all years. Statistical significance was tested with a bootstrapped MWU-test ($n = 1000$, $\alpha = 0.05$). Positive values show higher than average (all years) median WCI values indicating less severe water shortage conditions whereas negative values show lower than average (all years) median WCI values indicating more severe shortage conditions.

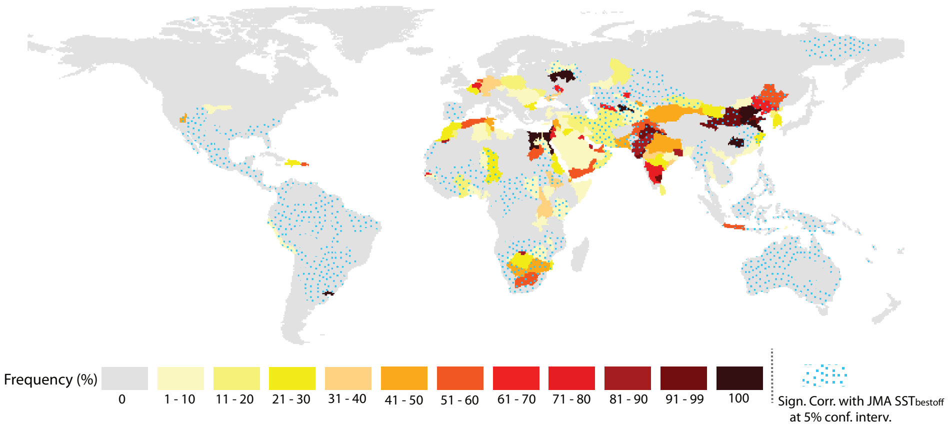

Figure A7. Frequency (%) of water shortage events (WCI) over the period 1961–2010.The blue dots indicate whether the water shortage conditions in an FPU are significantly correlated to variation to JMA $\text{SST}_{\text{bestoff}}$ at a 5 % confidence interval (tested using regular bootstrapping, $n = 1000$).

Title Page
Abstract Introduction
Conclusions References
Tables Figures
◂◂ ▸▸
◂ ▸
Back Close
Full Screen / Esc
Printer-friendly Version
Interactive Discussion

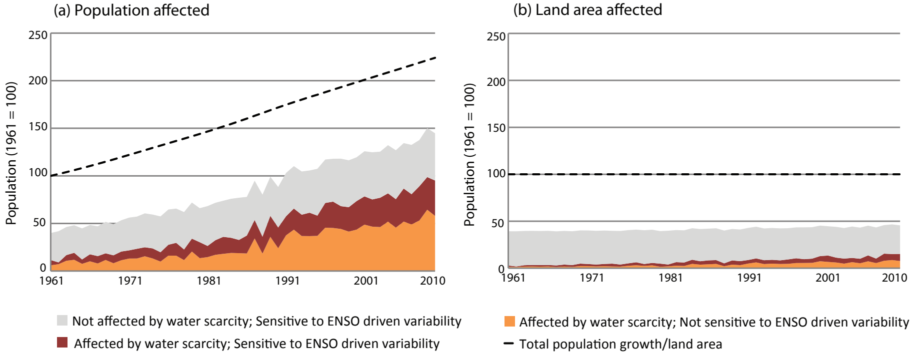

Figure A8. Increase in population and land area affected by either water scarcity events and/or ENSO driven climate variability over the period 1961–2010, as estimated with the WCI for water shortage conditions. **(a)** shows the growth in population living under water shortage events and/or living in areas sensitive to ENSO driven climate variability relative to the total growth in global population (set at 100 in 1961). **(b)** shows the increase in land area affected by either water shortage events and/or ENSO driven climate variability relative to the total global land area (100).

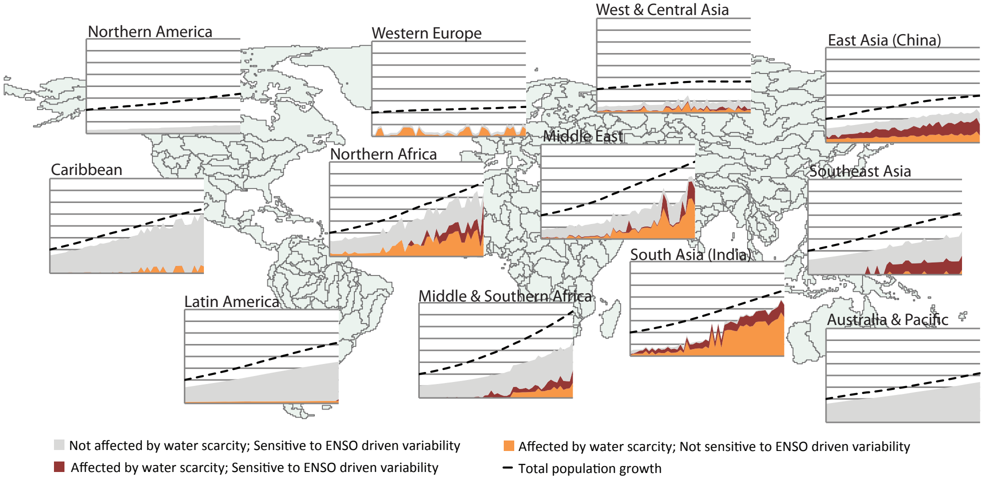

Figure A9. Regional variation in developments of population (%) affected by either water scarcity events and/or ENSO driven climate variability over the period 1961–2010, as estimated with the CTA-ratio for water shortage conditions. **(a)** shows per world region the growth in population living under water shortage events and/or living in areas sensitive to ENSO riven climate variability, relative to the growth in total global population (set at 100 in 1961). *Y* axis ranges from 0 up to 400.

(a) Consumption To Availability Ratio

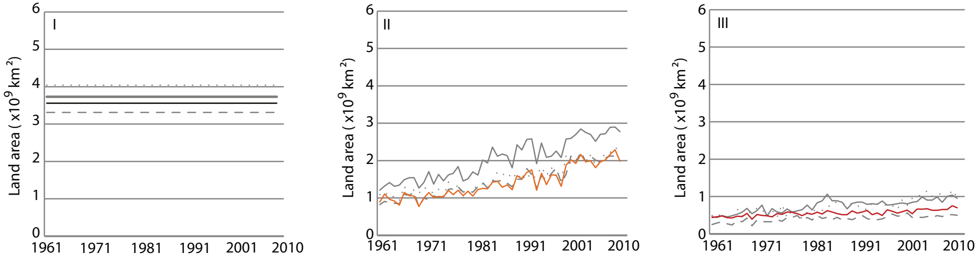

(b) Water Crowding Index

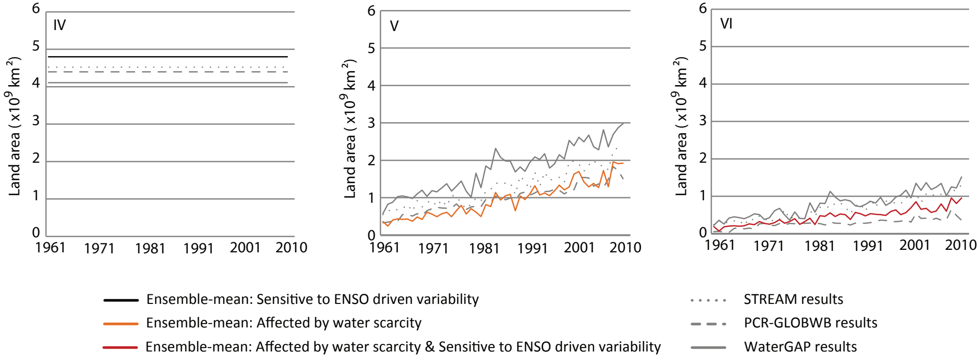

Figure A10. Developments in land area sensitive to ENSO driven climate variability and/or affected by water scarcity events as assessed by the individual global hydrological models (STREAM, PCR-GLOBWB, and WaterGAP) and the ensemble-mean. Figure A10.I and IV shows the development in land area sensitive to ENSO driven climate variability whilst Fig. A10.II and V gives the increase in land area affected by water stress and shortage events. Figure A10.III and VI visualizes the land area affected by water stress and shortage events with a significant correlation to ENSO driven climate variability.